

Lappeenranta University of Technology  
School of Engineering Science  
Degree Program in Computational Engineering and Technical Physics

Master's Thesis

**Alla Kliuzheva**

**THE MECHANICAL BEHAVIOR OF ORIENTED 3D FIBER  
STRUCTURES**

Examiners: Associate Professor Tuomo Kauranne  
Doctor of Philosophy Joonas Sorvari

Supervisors: Associate Professor Tuomo Kauranne  
Doctor of Philosophy Joonas Sorvari

# ABSTRACT

Lappeenranta University of Technology  
School of Engineering Science  
Degree Program in Computational Engineering and Technical Physics

Alla Kliuzheva

## **The mechanical behavior of oriented 3D fiber structures**

Master's Thesis

2017

51 pages, 47 figures, 5 tables.

Examiners: Associate Professor Tuomo Kauranne  
Doctor of Philosophy Joonas Sorvari

Keywords: static analysis, stress-strain state, structured material, fibers, material orientation

This paper is devoted to the study of mechanics of a structured material obtained from paper fibers. The object of investigation is a three-dimensional shell body in the form of a hemisphere. The purpose of this thesis is to study the mechanical behavior of a material based on structured fibers. It is proposed to create a three-dimensional geometric model from a single-layer and four-layer structured material in the finite element analysis package ABAQUS, release 6-14.1. Two types of boundary conditions, two types of loading and six variants of fiber orientation in the material were selected. It is expected that in each of the four cases (a combination of boundary conditions and load types) it will be possible to identify which of the fiber orientation options in the material shows the greatest resistance to mechanical deformation.

## ACKNOWLEDGEMENTS

I would like to express my deepest gratitude to my supervisor Doctor of Philosophy Joonas Sorvari for an interesting topic for Master's Thesis and excellent guidance throughout the course of this study. I also would like to thank him for new knowledge and practical skills given during this research work.

I would like to express my big gratitude to my supervisor Associate Professor Tuomo Kauranne for his excellent guidance and exact corrections both during Master's thesis writing and the whole year during the course 'Case study seminar'. Thank you for great and scientific atmosphere!

I would like to express my heart gratitude to Teemu Leppänen for his help, support and constant consulting during practical modeling of a problem and writing the thesis. His productive advice have helped to make clear a lot of complicated moments.

I would like to acknowledge the Lappeenranta University of Technology, the Department of Technomathematics, for hospitality and friendly atmosphere, useful possibilities provided for students, and also all staff of LUT for their willingness and desire to help in the process of education.

I would like to acknowledge the Southern Federal University, Institute of Mathematics, Mechanics and Computer Science, for given opportunity to study in LUT. In particular, I would like to express my gratitude to my Russian supervisor Associate Professor Mikhail Karyakin for his help and advice during my study.

Lappeenranta, June, 2017

Alla Kliuzheva

# CONTENTS

|          |   |           |
|----------|---|-----------|
| <b>1</b> | <b>INTRODUCTION</b>                                   | <b>6</b>  |
| 1.1      | About the selected material . . . . .                 | 6         |
| 1.2      | Objectives and delimitations . . . . .                | 7         |
| 1.3      | Research task . . . . .                               | 7         |
| 1.4      | Structure of the Thesis . . . . .                     | 8         |
| <b>2</b> | <b>THEORETICAL BACKGROUND</b>                         | <b>9</b>  |
| 2.1      | Stress and Strain concepts . . . . .                  | 9         |
| 2.2      | Strain-Displacement Relation . . . . .                | 12        |
| 2.3      | Governing equations . . . . .                         | 14        |
| 2.4      | Material model . . . . .                              | 14        |
| 2.5      | Constitutive equations of material behavior . . . . . | 16        |
| 2.6      | Finite element modeling approach . . . . .            | 17        |
| <b>3</b> | <b>IMPLEMENTATION</b>                                 | <b>24</b> |
| 3.1      | Paper fiber description . . . . .                     | 24        |
| 3.2      | Structure of ABAQUS script . . . . .                  | 26        |
| <b>4</b> | <b>RESULTS</b>  | <b>28</b> |
| 4.1      | One-layer structure analysis . . . . .                | 28        |
| 4.2      | Four-layer structure analysis . . . . .               | 38        |
| <b>5</b> | <b>CONCLUSIONS</b>                                    | <b>49</b> |
| <b>6</b> | <b>REFERENCES</b>                                     | <b>50</b> |

## ABBREVIATIONS AND SYMBOLS

|                        |                                |
|------------------------|--------------------------------|
| <b>1D</b>              | One-dimensional                |
| <b>2D</b>              | Two-dimensional                |
| <b>3D</b>              | Three-dimensional              |
| <b>FEM</b>             | Finite element method          |
| <b>FE</b>              | Finite element                 |
| $F_{subscript}$        | Force                          |
| $\sigma$               | Stress tensor                  |
| $\epsilon$             | Strain tensor                  |
| $\sigma_{subscript}$   | Stress component               |
| $\epsilon_{subscript}$ | Strain component               |
| $E$                    | Cauchy's strain tensor         |
| $e$                    | Green's's strain tensor        |
| $C_{subscript}$        | Tensor of elastic modulus      |
| $G$                    | Shear modulus                  |
| $\nu$                  | Poisson's ratio                |
| $E$                    | Young's modulus                |
| <b>ODE</b>             | Ordinary differential equation |
| <b>PDE</b>             | Partial differential equation  |
| $w_l$                  | Weight function                |
| $\tilde{u}$            | Approximate solution           |
| $N_i$                  | Form function                  |
| <b>MD</b>              | Machine direction              |
| <b>CD</b>              | Cross-machine direction        |
| $\theta$               | Orientation angle              |

# 1 INTRODUCTION

## 1.1 About the selected material

Paper is a popular material for many human purposes. It is used mostly for printing and packing. Studying mechanical properties of paper allows improve its quality and find new fields for application. The opportunity of recycling paper makes it an ecologically safe material.

Fibers are particles that form the network part of the paper structure. Controlling the fibers during the forming process, different kinds of structured material can be obtained. Changing the size, orientation and amount of fibers allows receiving various types of paper or cardboard. Some selected kinds of structured material from fibers are the main objects of study in this thesis.

Other materials can provide similar properties with paper so that mechanical properties of paper is a base for exploring structured material from fibers. Description of paper physics is studied in [1]. Mechanical behavior of paper is performed in [2]. Interesting characteristics of paper quality are density, thickness, amount of water in the final state, location of particles forming a paper or cardboard sheet [3]. It should be noticed, structured materials usually include several types of substances forming a structure. Thus, such kinds of materials can be considered as heterogeneous. Heterogeneity is one of basic characteristics of material, it means that a material is a mixture of substances in different states, or phases, for example, liquid and solid, liquid and viscous. Chemical and physical properties are different for substances in the mixture. The substances in the mixture also have a so-called surface of dividing [4]. The second available type of material, homogeneous, does not have any dividing surfaces between substances. This type of material has only one state (a phase) in composition or origin of substance.

The property of heterogeneity appears in this kind of materials from the paper making process, as it is noticed in [4, 5, 6]. Water, fibers, fillers, fines and air are the substances in what cannot be a completely homogeneous mixture. As heterogeneous material, structured material from fibers is a complex and interesting object.

As it is presented in [7], fiber orientation can be a significant characteristic of structured material. Models of fiber orientation are presented in [8]. The model presented by Lepänen in [7] is the basic model of fiber orientation in this thesis. The impact of thickness

is studied with varying a number of layers in the object from paper fibers.

Studying the mechanical behavior of the structure can be done by the finite element method. This approach is demonstrated in [8]. The finite element method is used by the author of the thesis for numerical analysis of the stress-strain state of the selected structured materials.

## **1.2 Objectives and delimitations**

The aim of this thesis is to study the mechanical behavior of structured fiber-based material. There are three research questions:

- How fiber distribution effects on mechanical behavior of structured fiber-based material?
- Can fiber orientation be used to decrease the deformation of the structure?
- How boundary conditions and loads affect the deformation of the structured material?

Moisture and density of paper are not studied in this thesis.

## **1.3 Research task**

There is a number of steps that are performed for the thesis:

1. Study the literature related with paper physics, continuum mechanics and fiber orientation model.
2. Create a one-layer model of structured material with respect to fiber orientation.
3. Apply several given types of fiber orientation.
4. Apply selected types of boundary conditions and load areas.
5. Run all the combinations of fiber orientations, boundary conditions and loads with some chosen value of pressure.

6. Create four-layer models on the base of one-layer structure.
7. Apply and execute all the combinations of a problem formulation from step 5 for new four-layer structures.
8. Present the results as graphs of dependency between value of pressure and displacement of a selected point in the structure.
9. Plot graphs of dependency between values of pressure and obtained stress distribution.
10. Analyze results.

## **1.4 Structure of the Thesis**

Chapter 2 contains theoretical material which describes stress and strain concepts, governing equations and constitutive model of material behavior. Finite element method (FEM) is also presented in this chapter. Chapter 3 introduces Abaqus environment as a tool for FEM and numerical analysis, includes the basic steps of modeling process and demonstrates the structure for Abaqus scripting on the Python programming language. Chapter 4 shows all the results obtained for one- and four-layer structure using Abaqus environment. The conclusion of the thesis is presented in Chapter 5. List of references is located after Chapter 5.

## 2 THEORETICAL BACKGROUND

### 2.1 Stress and Strain concepts

A state of any solid object can be described with basic concepts of structural mechanics: stress and strain. Let us consider the origin and formation of both of these processes in detail.

In structural mechanics, stress can be defined as a ratio of the force acting on a given area in a body to the area when the size tends to zero. The three-dimensional state of stress at a point in a stressed body may be described with respect to the stress arbitrarily chosen orthogonal planes passing through the point of origin. These planes are chosen normal to the Cartesian coordinate axes  $x_1, x_2, x_3$ . An infinitesimal cube whose sides are parallel to these planes can be considered. Figure 1 demonstrates the most general situation where forces  $F_1, F_2, F_3$  acting at some angle to each of the planes [9]. Figure 1 presents forces and stress components in an infinitesimal cube:

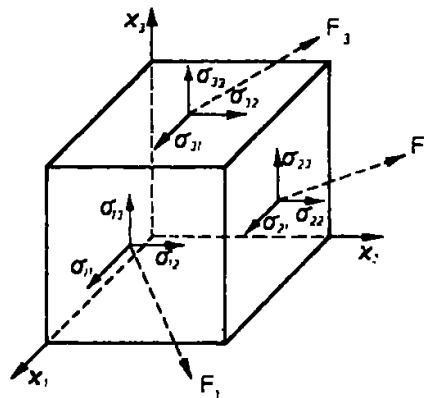


**Figure 1.** Forces and stress components [9].

Usually these forces are resolved into components parallel to the coordinate axes and we consider their stress components instead of the forces. A double subscript notation is applied to differentiate between the various components. The particular plane on which a stress component acts is named by the first subscript. The subscript 1 indicates that the stress acts on the normal to the  $x_1$  direction, the subscript 2 shows normality to  $x_2$  etc. The second subscript indicates the direction of the vector of the stress component under consideration. So that, if the right-hand face of the cube  $\sigma_{22}$  is a normal stress component

in the  $x_2$  direction,  $\sigma_{21}$  is a shearing component in the  $x_1$  direction,  $\sigma_{23}$  is a shearing component in  $x_3$  direction and all three components are acting on a plane perpendicular to the  $x_2$  axis [9].

The nine components forming in describing the states of stress form a second order Cartesian tensor, also called a stress tensor. The stress vector  $T_i$  is the force per unit area acting on the surface whose normal is defined by the unit vector  $n_j$ . The traction  $T_i$  is related with the stress tensor  $\sigma_{ij}$  by  $T_{ij} = \sigma_{ij}n_j$ . The nine components of the stress tensor may be written in matrix form as follows:

$$\sigma_{ij} = \boldsymbol{\sigma} = \begin{bmatrix} \sigma_{11} & \sigma_{12} & \sigma_{13} \\ \sigma_{21} & \sigma_{22} & \sigma_{23} \\ \sigma_{31} & \sigma_{32} & \sigma_{33} \end{bmatrix} \quad (1)$$

where the symbol  $\sigma_{ij}$  employs a subscript notation in which dummy subscript  $i$  and  $j$  are understood to take values of 1, 2, 3 as indicated in the matrix on the right-hand side [9].

Summation convention can be noticed as another rule related with the subscript notation. When a letter subscript is repeated in a given term of an equation as in  $\sigma_{ii}$  or  $\sigma_{ij}a_j$  it is to be understood that this symbol represents the sum of three terms formed by substituting 1, 2, 3 for the repeated subscript [9]. The stress tensor can be divided into two parts, a mean normal stress tensor and deviatoric stress tensor:

$$\sigma_{ij} = \begin{bmatrix} \sigma_{11} & \sigma_{12} & \sigma_{13} \\ \sigma_{21} & \sigma_{22} & \sigma_{23} \\ \sigma_{31} & \sigma_{32} & \sigma_{33} \end{bmatrix} = \begin{bmatrix} \sigma_v & 0 & 0 \\ 0 & \sigma_v & 0 \\ 0 & 0 & \sigma_v \end{bmatrix} + \begin{bmatrix} s_{11} & s_{12} & s_{13} \\ s_{21} & s_{22} & s_{23} \\ s_{31} & s_{32} & s_{33} \end{bmatrix} \quad (2)$$

as well as

$$\sigma_{ij} = \sigma_v \delta_{ij} + s_{ij}, \quad (3)$$

where  $\delta_{ij}$  is Kronecker delta.

Choosing  $\sigma_v$  to be an average normal stress of the stress tensor  $\sigma_{ij}$ ,

$$\sigma_v = \frac{1}{3} \sigma_{kk} = \frac{1}{3} (\sigma_{11} + \sigma_{22} + \sigma_{33}), \quad (4)$$

where  $\sigma_{kk}$  makes use of the summation convention. The average normal stress sigma may be shown to be independent of the choice of the coordinate axes [9]. Deviatoric stress can be written as:

$$s_{ij} = \sigma_{ij} - \frac{1}{3} \sigma_{kk} \delta_{ij} \quad (5)$$

and

$$s_{ij} = \begin{bmatrix} s_{11} & s_{12} & s_{13} \\ s_{21} & s_{22} & s_{23} \\ s_{31} & s_{32} & s_{33} \end{bmatrix} = \begin{bmatrix} \sigma_{11} - \sigma_v & \sigma_{12} & \sigma_{13} \\ \sigma_{21} & \sigma_{22} - \sigma_v & \sigma_{23} \\ \sigma_{31} & \sigma_{32} & \sigma_{33} - \sigma_v \end{bmatrix} \quad (6)$$

respectively. It can be shown that the sum of the normal deviatoric stress components  $s_{ii}$  is zero if as assumed  $\sigma_v$  is the average of the normal components of  $\sigma_{ij}$ . That is

$$s_{11} + s_{22} + s_{33} = 0. \quad (7)$$

Division of the state of stress into a volume stress component and deviatoric component is often convenient because of differences in mechanical behavior of materials under volumetric stressing in which there are no shearing stresses versus states of stress involving shearing stress [9].

Strain is a measure of the intensity of deformation at a point. Linear strain is the change in length of a line segment per unit of length as the length of the line segments becomes infinitesimal. Engineering shear strain is the change in angle at the point of intersection of two lines originally at right angles. To describe the state of strain at a point consider the change in configuration of a deformed body. The deformation of the body can be described by the functional relation between the undeformed and the deformed states. Figure 2 shows how points positions change during a process of deformation:

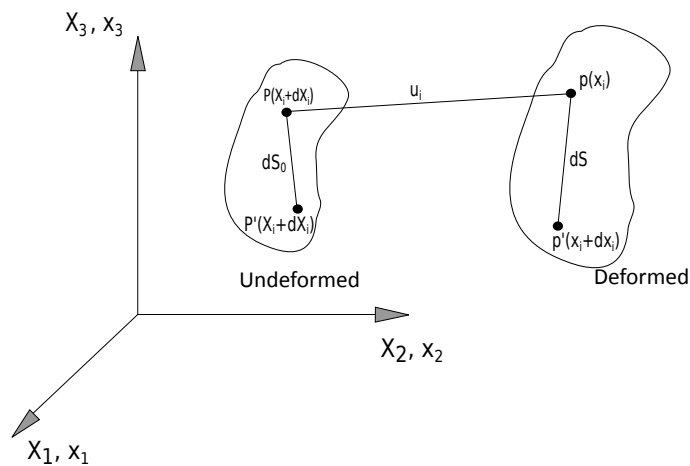


**Figure 2.** Deformation.

Consider the position of a point  $P$  and a neighboring point  $P'$  both in the undeformed state of a body. The positions of  $P$  and  $P'$  are described by fixed rectangular Cartesian coordinates  $X_i$  and  $X_i + \Delta X_i$  respectively, where  $i = 1, 2, 3$ . After deformation takes place, at time  $t$  the material points  $P$  and  $P'$  deform into  $p$  and  $p'$  where the position of  $p$  and  $p'$  are described the same coordinate system by  $x_i$  and  $x_i + \Delta x_i$  ( $i = 1, 2, 3$ ). The deformation of the body is assumed to be continuous and can be described by the functional dependence of  $X_i$  and  $X_i + \Delta X_i$  and  $t$ :

$$x_i = x_i[X, t]. \quad (8)$$

The deformation from  $P$  to  $p$  is the difference between the square of the length elements:

$$(ds)^2 - (ds_0)^2 = \left( \frac{\partial x_i}{\partial X_k} \frac{\partial x_i}{\partial X_l} - \delta_{kl} \right) dX_k dX_l = 2E_{kl} dX_k dX_l. \quad (9)$$

or

$$(ds)^2 - (ds_0)^2 = \left( \delta_{kl} - \frac{\partial X_i}{\partial x_k} \frac{\partial X_i}{\partial x_l} \right) dx_k dx_l = 2e_{kl} dx_k dx_l \quad (10)$$

These formulas contain Green's strain tensor and Cauchy's strain tensor, they are denoted as  $E_{kl}$  and  $e_{kl}$  respectively:

$$E_{kl} = \frac{1}{2} \left( \frac{\partial x_i}{\partial X_k} \frac{\partial x_i}{\partial X_l} - \delta_{kl} \right) \quad (11)$$

$$e_{kl} = \frac{1}{2} \left( \delta_{kl} - \frac{\partial X_i}{\partial x_k} \frac{\partial X_i}{\partial x_l} \right) \quad (12)$$

In the former, the strain is measured with respect to the undeformed state (gauge length in uniaxial strain); in the latter it is measured with respect to the deformed state (sometimes called the true strain for uniaxial strain). These two tensors are symmetric with respect to the coordinates [9].

## 2.2 Strain-Displacement Relation

The displacement vector  $u_i$  is defined by

$$u_i(X, t) = x_i(X, t) - X_i \quad (13)$$

or

$$u_i(x, t) = x_i - X_i(x, t) \quad (14)$$

where  $X$  and  $x$ , representing  $X_1, X_2, X_3$  and  $x_1, x_2, x_3$  respectively, are the coordinates of the point. All three coordinates of the point appear in the expression for each value of  $i$  in  $u_i$ . Inserting  $u_i$  for  $x$  and  $X_i$  into strain tensor representations, we can obtain the following simplification:

$$E_{ij} = \frac{1}{2} \left[ \frac{\partial u_i}{\partial X_j} + \frac{\partial u_j}{\partial X_i} + \frac{\partial u_\alpha}{\partial X_i} \frac{\partial u_\alpha}{\partial X_j} \right] \quad (15)$$

$$e_{ij} = \frac{1}{2} \left[ \frac{\partial u_i}{\partial x_j} + \frac{\partial u_j}{\partial x_i} + \frac{\partial u_\alpha}{\partial x_i} \frac{\partial u_\alpha}{\partial x_j} \right] \quad (16)$$

If the components of displacement  $u_i$  are such that their first derivatives are so small that the products of the partial derivatives of  $u_i$  in the third term are negligible compared to the first two terms, then Cauchy's strain tensor reduces to Cauchy's infinitesimal strain tensor,

$$\varepsilon_{ij} = \frac{1}{2} \left[ \frac{\partial u_i}{\partial x_j} + \frac{\partial u_j}{\partial x_i} \right]. \quad (17)$$

In ordinary notation ( $x, y, z$  for  $x_1, x_2, x_3$ ;  $u, v, w$ , for  $u_1, u_2, u_3$ ) the components of  $\varepsilon_{ij}$  become as follows:

$$\begin{aligned} \varepsilon_{xx} &= \frac{\partial u}{\partial x}, \varepsilon_{xy} = \frac{1}{2} \left( \frac{\partial u}{\partial x} + \frac{\partial v}{\partial y} \right) = \varepsilon_{yx} \\ \varepsilon_{yy} &= \frac{\partial v}{\partial y}, \varepsilon_{xz} = \frac{1}{2} \left( \frac{\partial u}{\partial z} + \frac{\partial w}{\partial x} \right) = \varepsilon_{zx} \\ \varepsilon_{zz} &= \frac{\partial w}{\partial z}, \varepsilon_{yz} = \frac{1}{2} \left( \frac{\partial v}{\partial y} + \frac{\partial w}{\partial z} \right) = \varepsilon_{zy} \end{aligned} \quad (18)$$

In the case of infinitesimal displacement, the distinction between Green's and Cauchy's strain tensor disappears, since then it is immaterial whether the derivatives of displacement are with respect to deformed or undeformed coordinates [9].

The nine components of the strain tensor  $\varepsilon_{ij}$  comprise a second order Cartesian tensor whose matrix is as follows:

$$\varepsilon_{ij} = \boldsymbol{\varepsilon} = \begin{bmatrix} \varepsilon_{11} & \varepsilon_{12} & \varepsilon_{13} \\ \varepsilon_{21} & \varepsilon_{22} & \varepsilon_{23} \\ \varepsilon_{31} & \varepsilon_{32} & \varepsilon_{33} \end{bmatrix}, \quad (19)$$

where the subscript notation has the same significance as in the stress tensor except that its relationship to engineering strain is not as direct as for stress. The strain tensor is also symmetrical about the diagonal line from  $\varepsilon_{11}$  to  $\varepsilon_{33}$ .

## 2.3 Governing equations

Consider the static equilibrium state of a body. When stresses act on the body surface, they differ as normal stresses (act perpendicularly to the surface) and shear stresses (all the other terms). Body forces such as gravity, magnetic and centrifugal forces exist in the body as well. Body forces can depend on the position in the body and can change with time. The static equilibrium state of the body requires that the sum of all forces along a coordinate direction (the resultant) should be equal to zero. For  $x_1$  direction the equilibrium equation contains the sum all the forces acting on the element in this direction. The forces are obtained by multiplying the stress by the area on which the stress acts:

$$\begin{aligned} & \left( \sigma_{11} + \frac{\partial \sigma_{11}}{\partial x_1} \right) dx_2 dx_3 - \sigma_{11} dx_2 dx_3 + \left( \sigma_{21} + \frac{\partial \sigma_{21}}{\partial x_2} \right) dx_1 dx_3 - \sigma_{21} dx_1 dx_3 \\ & + \left( \sigma_{31} + \frac{\partial \sigma_{31}}{\partial x_3} \right) dx_1 dx_2 - \sigma_{31} dx_1 dx_2 + F_1 dx_1 dx_2 dx_3 = 0. \end{aligned} \quad (20)$$

The other two equilibrium equations are obtained it the same way. After dividing the equations by  $dx_1 dx_2 dx_3$  the three equations oriented along the coordinate axes:

$$\begin{aligned} \frac{\partial \sigma_{11}}{\partial x_1} + \frac{\partial \sigma_{21}}{\partial x_2} + \frac{\partial \sigma_{31}}{\partial x_3} + F_1 &= 0 \\ \frac{\partial \sigma_{12}}{\partial x_1} + \frac{\partial \sigma_{22}}{\partial x_2} + \frac{\partial \sigma_{32}}{\partial x_3} + F_2 &= 0 \\ \frac{\partial \sigma_{13}}{\partial x_1} + \frac{\partial \sigma_{23}}{\partial x_2} + \frac{\partial \sigma_{33}}{\partial x_3} + F_3 &= 0 \end{aligned} \quad (21)$$

Equations written in the tensor form:

$$\frac{\partial \sigma_{ij}}{\partial x_i} + F_j = 0, (i, j = 1, 2, 3) \quad (22)$$

## 2.4 Material model

In general meaning, elasticity is the ability of a body to resist a destructive influence or deforming force and to return to its original size and shape when that influence or force is removed [9]. Linear elasticity studies relationships between stress and strain when deformation has linear dependency on loads. In that case, there is so called "ideal elasticity" of a body. Wood, glass, aluminium, steel and cast iron are materials with this ability. Generalized Hooke's law establishes a proportional relationship between stress

and strain tensor:

$$\sigma_{ij} = C_{ijkl}\varepsilon_{kl}, \quad (23)$$

where  $C_{ijkl}$  is a tensor of elastic modulus.

Shear modulus  $G$  and Poisson's ratio  $\nu$  (the signed ratio of transverse strain to axial strain) also are important characteristics of an elastic body. There is a relation between shear modulus  $E$  (Young's modulus), the elastic modulus and the Poisson's ratio:

$$G = \frac{E}{2(1 + \nu)} \quad (24)$$

A model of linear elastic body is widely used in calculation stress and strain distribution when a body has static or quasistatic state with acting forces [9].

Consider Figure 3, it demonstrates a typical process of generalized material deformation. The domain  $OA$  represents linear elasticity, stress and strain are proportional to each other. Here  $\sigma_{prop}$  is a maximum stress value when Hooke's Law holds.  $AB$  is an area of nonlinear elasticity, it means that a body can have large deformations when small loads act. The elastic limit  $\sigma_{el}$  is a value when the body loses the ability of restoring after load. The  $BC$  area is shows the ability of fluidity: the body continues to experience deformation without increasing load. With further increase in the load, the body regains its ability to resist deformation at  $CD$ . The stress increases, reaches the maximum at point  $D$ , which corresponds to the beginning of the destruction. Section  $DE$  corresponds to the gradual destruction of bodies [10].

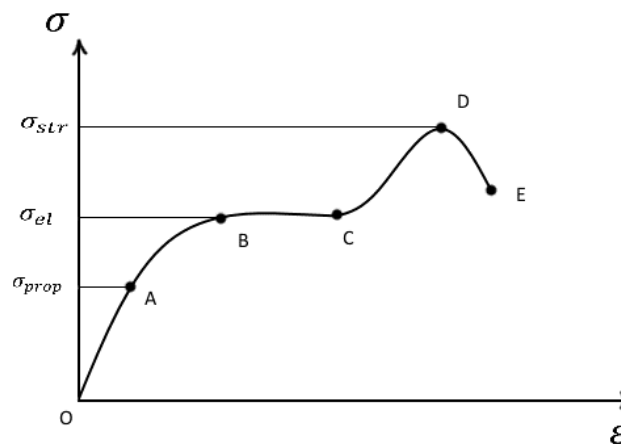


**Figure 3.** Stress-strain curve.

One more characteristics defining the material is the dependency of mechanical properties on direction of applied load. The first kind, isotropic material has the same properties in all the directions. Examples of isotropic materials are glass and many metals. Hooke's Law for isotropic material can be expressed as:

$$\sigma_{ij} = \frac{E\nu}{(1+\nu)(1-2\nu)}\varepsilon_{kk}\delta_{ij} + \frac{E}{(1+\nu)}\varepsilon_{ij}. \quad (25)$$

The material which has different characteristics applying loads in different directions, is called anisotropic. Examples are wood and composites. Orthotropic material is a special case of anisotropic material, in such a material the mechanical properties changes along three mutually orthogonal coordinate axes [9].

## 2.5 Constitutive equations of material behavior

Paper fiber can be considered as planar orthotropic lamina. The behavior of planar orthotropic lamina can be presented with stiffness matrix [11]:

$$\begin{Bmatrix} \sigma_1 \\ \sigma_2 \\ \tau_{12} \end{Bmatrix} = \begin{bmatrix} Q_{11} & Q_{12} & 0 \\ Q_{12} & Q_{22} & 0 \\ 0 & 0 & Q_{66} \end{bmatrix} \begin{Bmatrix} \epsilon_1 \\ \epsilon_2 \\ \gamma_{12} \end{Bmatrix} \quad (26)$$

and compliance matrix:

$$\begin{Bmatrix} \epsilon_1 \\ \epsilon_2 \\ \tau_{12} \end{Bmatrix} = \begin{bmatrix} S_{11} & S_{12} & 0 \\ S_{12} & S_{22} & 0 \\ 0 & 0 & S_{66} \end{bmatrix} \begin{Bmatrix} \sigma_1 \\ \sigma_2 \\ \tau_{12} \end{Bmatrix} \quad (27)$$

where

$$\begin{aligned} Q_{11} &= \frac{S_{22}}{S_{11}S_{22} - S_{12}^2} \\ Q_{22} &= \frac{S_{11}}{S_{11}S_{22} - S_{12}^2} \\ Q_{12} &= \frac{S_{12}}{S_{11}S_{22} - S_{12}^2} \\ Q_{66} &= \frac{1}{S_{66}} \end{aligned} \quad (28)$$

In natural axes the compliance tensor components for orthotropic lamina using Cartesian axes of coordinates are formed as:

$$\begin{aligned}
 S_{11} &= \frac{1}{E_y} \\
 S_{22} &= \frac{1}{E_x} \\
 S_{12} &= -\frac{\nu_{yx}}{E_y} = -\frac{\nu_{xy}}{E_x} \\
 S_{66} &= \frac{1}{G_{yx}}
 \end{aligned} \tag{29}$$

The stiffness tensor components for orthotropic lamina using Cartesian axes of coordinates are formed as:

$$\begin{aligned}
 Q_{11} &= \frac{E_y}{1 - \nu_{yx}\nu_{xy}} \\
 Q_{22} &= \frac{E_x}{1 - \nu_{yx}\nu_{xy}} \\
 Q_{12} &= \frac{\nu_{yx}E_x}{1 - \nu_{yx}\nu_{xy}} = \frac{\nu_{xy}E_y}{1 - \nu_{yx}\nu_{xy}} \\
 Q_{66} &= G_{yx}
 \end{aligned} \tag{30}$$

## 2.6 Finite element modeling approach

Finite element method (FEM) is a numerical method for solving differential equations, as well as integral equations that arise in the solution of applied physics and mathematics problems. The method is widely applied to solve the problems of mechanics of a deformable solid body, heat transfer, hydrodynamics and electrodynamics [8]. Finite element method appeared from necessity to solve complex problems in area of structural mechanics and theory of elasticity approximately in 1930s. A. Hrennikov and R. Courant provided the first developments in the early 1940s. Hrennikoff's work demonstrated the discretization of a domain by using a lattice analogy. Courant's approach divided the area into finite triangular subregions to solve second order elliptic partial differential equations (PDEs). Courant's contribution was evolutionary, based on a large amount of earlier results for PDEs developed by Rayleigh, Ritz, and Galerkin [12, 13].

Further development of the finite element method relates to the solution of the problems for space research in the 1950s. The finite element method become fast-developing in the 1960s and 1970s with the research of J. H. Argyris with co-workers at the University of Stuttgart, R. W. Clough with co-workers at UC Berkeley, O. C. Zienkiewicz with co-

workers Ernest Hinton, Bruce Irons and others at the University of Swansea, Philippe G. Ciarlet at the University of Paris 6 and Richard Gallagher with co-workers at Cornell University. A rigorous mathematical basis to the finite element method was provided in 1973 with the publication by Strang and Fix [13]. The method has been generalized for the numerical modeling of physical systems in a wide variety of engineering disciplines such as electromagnetism, heat transfer, and fluid dynamics. The process of finite element analysis involves a certain sequence of steps [14]:

1. Discretization of the domain: the construction of a grid, the specification of the material properties for the elements. The area of the problem is approximated (covered) by disjoint sub-regions of a simple type, which are called finite elements (FE). The set of elements for the region is called a finite element mesh. The vertices of the FE are called nodes. Nodes are designed to describe the geometry of the element and to specify the solution components (an unknown value is specified in the nodes). Nodes can be external and internal. External nodes are located on the boundary of the element and are used to connect the elements to each other. Also, the nodes can lie between the corner nodes. Element can have internal nodes; such elements provide a more accurate description of the required functions.

The components of a solution at a node are called degrees of freedom. Depending on the considered problems, the number of degrees of freedom in the node varies. For example, if the heat conduction problem is considered, at each point one temperature value is sought-one degree of freedom. On the other hand, if we consider the two-dimensional elasticity problem with respect to unknown displacements, then the number of components will be equal to two, since the displacement is a vector quantity  $u = (u_x, u_y)$ . As the degrees of freedom, both the node values of the unknown function and its derivatives with respect to the spatial coordinates at the nodes can appear. In addition, it should be specified the properties of the material from which the construction or FE is made. For example, for isotropic bodies, when solving problems in the theory of elasticity, one must know constants such as the Young's modulus and the Poisson's ratio of the material.

2. Selection of approximating (basic) functions. Most often, the basic functions are chosen in the form of polynomials. Therefore, the space on which the solution is sought is the space of piecewise polynomial functions. Basic functions can have a different order: linear, quadratic, cubic, etc.

3. Formation of ODE system with contributions from elements and nodes, the boundary conditions in the system of equations. For example, if the problem is solved using the

Galerkin method (the weighted residual method), integrals are formed from the product of the discrepancy into weight functions, which are then equated to zero. If the problem is solved in a variational formulation using the Ritz method of minimizing the functional, then an ODE system is obtained after equating the derivatives of the functional to zero. The integrals over the domain are divided into integrals over the elements

$$\int_V w_l R dV = \sum_{e=1}^M \int_{V^e} w_l R dV \quad (31)$$

Elemental matrices and element vectors forming the global matrix (stiffness matrix) and the vector of the right sides of the system are calculated. The number of equations should be equal to the number of unknown values in the nodes on which the solution of the original system is sought, which is directly proportional to the number of elements and is limited only by the capabilities of the computer.

4. Solution of the system of equations.

5. Determination of design values in the elements. These quantities are usually derived from an unknown function (e.g, strain, voltage, heat flux, speed). The exact solution of the differential equation under substitution in the differential equation turns it into an identity at each point. The FEM solution assumes that the approximate solution  $\tilde{u}$  will satisfy the differential equation at the grid nodes  $\tilde{u}(x_i) = u(x_i) = u_i$  [14]. Figure 4 presents an example of a domain, divided by finite elements:

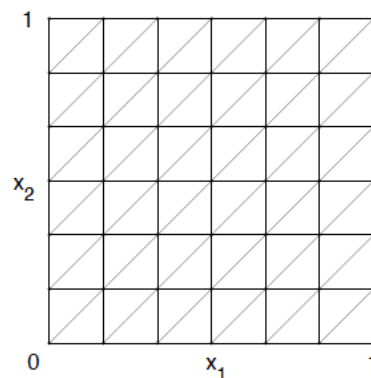


**Figure 4.** A domain divided into triangular subregions [15].

Consider the definition of piecewise linear basis functions. Basic functions are also called form functions. For example, consider form functions of the first order for one-dimensional finite element. The interval is divided with nodes  $x_1, \dots, x_n$  into finite ele-

ments  $e_k = (x_k, x_{k+1})$ ,  $k = 1, \dots, n-1$ , where  $h_k = x_{k+1} - x_k$  is the length of the element (grid size) [10]. For every inner node  $x_i$  a piecewise function can be written as follows:

$$N_i(x) = \begin{cases} 0, & x \leq x_{i-1} \\ \frac{x-x_{i-1}}{h_{i-1}}, & x_{i-1} \leq x \leq x_i \\ \frac{x_{i+1}-x}{h_i}, & x_i \leq x \leq x_{i+1} \\ 0, & x \geq x_{i+1} \end{cases}, \quad i = 2, \dots, n-1. \quad (32)$$

For boundary nodes  $x_1, x_n$  the form functions have the form:

$$N_1(x) = \begin{cases} \frac{x_2-x}{h_1}, & x_1 \leq x \leq x_2 \\ 0, & x \geq x_2 \end{cases}, \quad N_n(x) = \begin{cases} \frac{x-x_{n-1}}{h_{n-1}}, & x_{n-1} \leq x \leq x_n \\ 0, & x \leq x_{n-1} \end{cases} \quad (33)$$

Examples of form functions are presented by Figures 5 and 6:

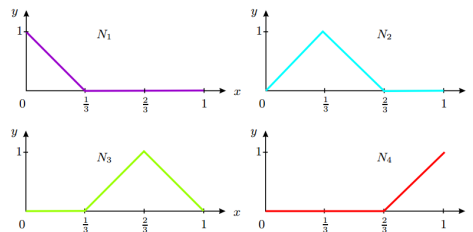


**Figure 5.** Form functions for a region of three elements [14].

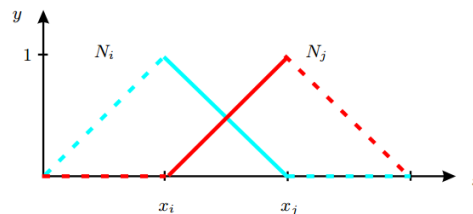


**Figure 6.** Form functions  $N_i, N_j$  for an element  $[x_i, x_j]$  [14].

Thus, the approximated function is represented in the form

$$\tilde{u} = \sum_i \alpha_i N_i(x), \quad (34)$$

where coefficients  $\alpha_i$  are found from the solved ODE system.

Important properties of form functions:

1. Form function  $N_i$  is equal to one in the node  $x_i$  and zero in the all other nodes.
2. Form function  $N_i$  is not equal to zero only for the elements which contain the node  $x_i$ .

Using these properties and the fact that the solution should satisfy the equation in the nodes, coefficients  $\alpha_i$  are function values in the nodes  $\alpha_i = u_i$ , so that

$$\tilde{u} = \sum_i u_i N_i(x). \quad (35)$$

Calculated values of form functions construct the stiffness matrix (or Dirichlet matrix). Such an approach to form the global finite element objects from the element objects is called an assembling procedure. In most cases the stiffness matrix is sparse. The sparse property allows to get fast and effective solution using special algorithms. In general case, elements of the stiffness matrix  $A^k$  can be written as the follow expression:

$$A_{ij} = \int_{\Omega} \nabla N_i \cdot \nabla N_j dx, \quad (36)$$

where  $\Omega$  is a space and  $N_i, N_j$  are basis functions defined on this space. Further on these matrices, the boundary conditions are superimposed and the system of differential equations is solved [14].

There are ways to improve accuracy of the solution. Grid size can be varied as well finite elements of higher order can be applied. In the latter case form functions are nonlinear.

Figure 7 presents examples of form function for one-dimensional finite element:

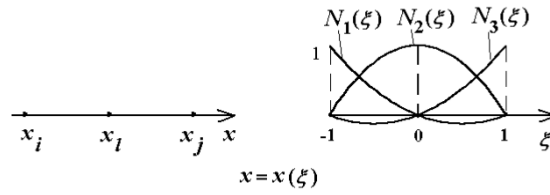


**Figure 7.** Form functions for a quadratic 1D finite element [16].

FEM can be considered also as an optimization approach. After discretization, there is an energy functional, which consists of all the energies associated with the specific finite element model. The finite element energy functional should be equal to zero, it is based on the law of conservation of energy. The finite element method reach the suitable solution for any finite element model by minimizing the energy functional. The minimum of this functional is detected by setting the derivative of the functional with respect to the unknown grid point potential for zero [17].

Some types of linear finite elements are presented on Figure 8:

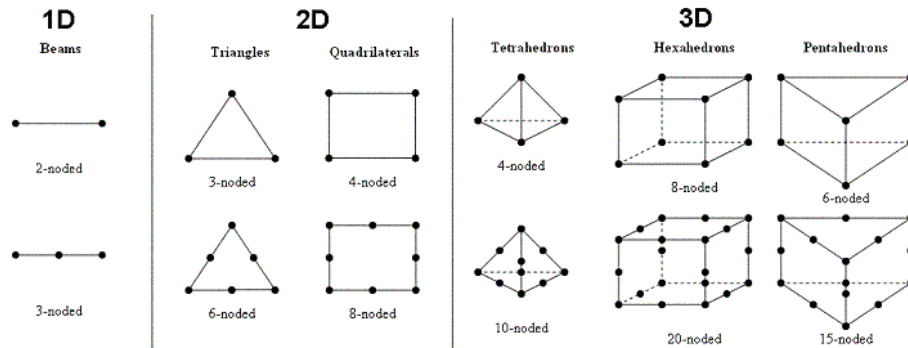


**Figure 8.** Linear finite element types [18].

Thus, the basic equation for finite element analysis is

$$\frac{dF}{dp} = 0, \tag{37}$$

where  $F$  is the energy functional and  $p$  is the unknown grid point potential to be calculated. In mechanics, the potential is displacement. This fact is based on the principle of virtual work, which states that if a particle is under equilibrium, under a set of a system of forces, then for any displacement, the virtual work is zero. Each finite element will have its own unique energy functional [17].

Today finite element analysis is the most powerful computational tool for structural verification and analysis of multi-physic problems. Numerical methods of research now provide for the application of a computer for the whole process of calculation, that is, from entering information about the geometry and topology of the structure, its physical properties and loads into the system, until the final results of the stress-strain states are obtained. With respect to the calculation of structures, the finite element method (FEM) is the most effective, very convenient computational method for solving applied problems of the mechanics of a deformable solid. FEM became also a fundamental method of mechanics for determining the stress-strain state of complex engineering structures. The advantage of FEM is its versatility in the computational technique when using different finite elements in the design model. Finite element models of various designs can be reduced to rod, plate, shell or bulk systems, which are under the influence of arbitrary loads. FEM makes it possible to calculate complex engineering structures from unified positions, i.e., in the possibility of forming flat and spatial design models based on rod and flat finite element, since the matrix apparatus of the method is of a standard nature for various shapes of elements. Modern finite element packages provide computational power for various size of grid. These packages are ANSYS, COMSOL, ABAQUS, and others [8, 12, 13].

### 3 IMPLEMENTATION

#### 3.1 Paper fiber description

The properties of paper fibers are considered in this section. In general, a brief description of the process of formation of a structured material is:

- The laying of fibers by several layers on some form of wire (in this work a hemispherical shape is used) using air flow;
- the compaction of the structure by pressing

Let us assume that the coordinate system is given from papermaking terminology. So, it can be denoted that  $x_1$  is MD (machine direction),  $x_2 = CD$  (cross machine direction) and  $x_3 = z$  (thickness direction). Machine direction is the direction of paper belt travel during depositing a fiber-and-water slurry onto a moving wire belt. Cross-machine direction is the perpendicular direction. Usually fibers tends to align their position in the machine direction. Cross-machine direction tests are frequently made during paper production to ensure that the papermaking furnish is being delivered across the forming wire with uniform thickness, consistency, moisture content, etc. Variations in CD profiles affect the quality, printability and runnability of the paper that will ultimately form [5].

Figure 9 demonstrates 2D model of fiber orientation used in the analysis:

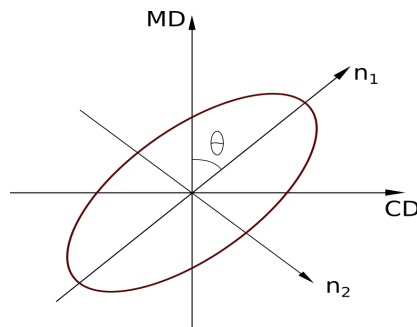


**Figure 9.** Orientation angle  $\Theta$  is the angle between MD-direction and the direction where the maximum of the fiber orientation distribution occurs [7].

Fibers in the structure are located chaotically but there is a main direction which can

be defined. Factors affecting the mechanical behavior of this type of material and their meanings used in this paper:

- The number of structured layers. It is considered a hemisphere from 1 and 4 layers, the structure has thickness 1 mm in both cases.
- Type of the material (isotropic, anisotropic). Some selected materials are tested. Firstly, an isotropic material defined by Young's modulus and Poisson's ratio for this type of the material. Further, orthotropic material of different types is considered. For the orthotropic material, Young's modulus, shear modulus and Poisson's ratio for two directions are used.
- An angle  $\theta$  (for anisotropic material). Orthotropic material is used with 0, 45 and 90-degree orientation angle. Moreover, Gaussian distribution of fiber directions is used for 0 and 90 degrees.
- Boundary conditions. Two types of boundary conditions are considered (Figure 10). The coordinate system for the whole object is Cartesian  $(x, y, z)$ . A fixed upper point of semisphere with coordinates  $(0, y, 0)$  is defined. Also the bottom edge of semisphere is fixed; every point has coordinates  $(x, z, 0)$ . The first type of boundary conditions is zero displacements on the bottom edge of semisphere, no rotation as well. The second type is zero displacements for y-axis on the bottom edge, and zero displacements of the upper point for x- and z-axes, zero rotations for the upper point.

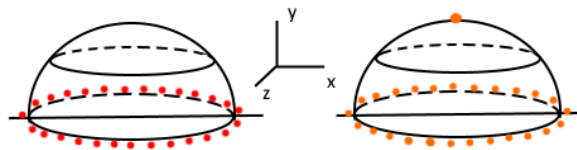


**Figure 10.** Boundary conditions. The left picture denotes the first type, the right illustrates the second type

- Type of loads. Two types of loads are considered. The first type is applying the distributed pressure on the whole surface. For the second type only upper part of the surface is used. Pressure is distributed on the upper part of the surface. These are illustrated on Figure 11.

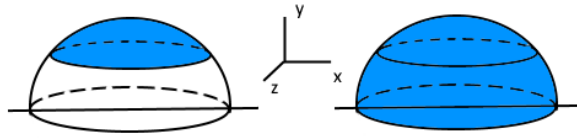


**Figure 11.** Load. The left picture denotes the first type, the right illustrates the second type

- Magnitude of load. Since the process of deformation is of interest to analysis before the buckling process, after testing different numerical values of the load, a pressure of 0.4 MPa was chosen.

### 3.2 Structure of ABAQUS script

ABAQUS environment is an effective tool for finite element modelling. ABAQUS allows taking into account all necessary aspects and setting different types of loads and boundary conditions. There are two styles of work with this program: interactive environment and scripting. The first approach offers step by step definition of model description and its characteristics and step by step execution of commands as well. Scripting favors writing of code that can be saved and used many times. Python is the language of ABAQUS scripting [19]. The following structure of ABAQUS script was used for the current type of a problem:

1. Constants.  
Any variables can be defined before the main part of the script. They can be used in any part after the definition.
2. Definition of geometry.  
We obtain the sketch and volume of the surface by rotation of an arc by 360 degree.
3. Define the material and sections.  
Young's modulus, shear modulus and Poisson's ratio are specified here.
4. Meshing.  
Define the size for finite element and mesh all the surface. The used size of element is equal to 0.8 mm, the type of elements is QUAD-DOMINATED. It means finite elements are quadratic mostly but triangular elements are allowed as well.
5. Assembling.

6. Material orientation.

In this part, an angle or distribution for the elements it is defined. We set a fixed angle of either 0, 45 or 90 degrees, and then a Gaussian distribution of angles with a mean of either 0 or 90 degrees. In both of these latter two cases the standard deviation of random angles is 5 degrees. To except accidental effects, an angle or distribution is defined on each element.

7. Composite layers (for many-layer structure).

8. Nonlinearity.

It is taken into account that nonlinear effects can exist during the deformation. It is allowed to calculate these effects. Since the form of the model is nonlinear, the calculations take into account the geometric nonlinearity.

9. Boundary conditions.

It is chosen to use areas/edges to set boundary conditions. Sets can be used for definition.

10. Loads.

Area, magnitude and direction of load are specified in this section.

11. Job.

All the sections above are collected to the 'Job' with special name. The Job can be saved and submitted that means start for analysis [19].

## 4 RESULTS

The simulated results are considered in this chapter. The stages of the process can be called as unloaded state, start of loading and end of loading. If the magnitude of load is large buckling may occur. The state before buckling is considered and analyzed. Four different cases were formed for finite element analysis. They are presented by Figure 12: As

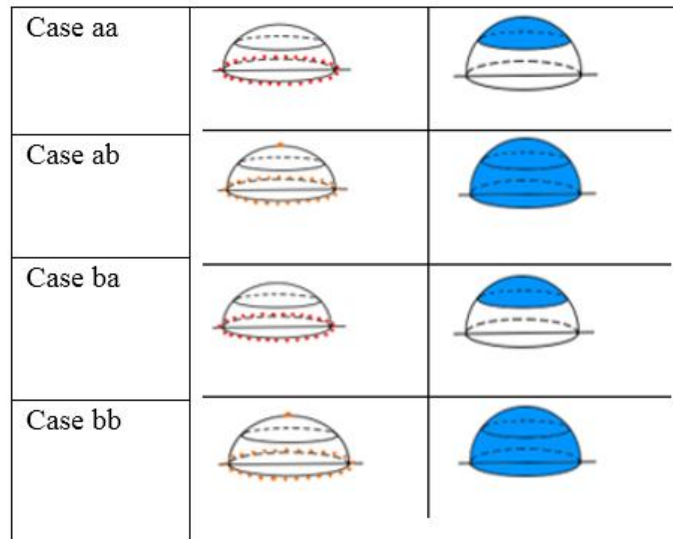


**Figure 12.** Combinations of boundary conditions and loads.

a result of calculations the dependency between displacement and pressure magnitudes is presented for different cases and types of material. Von Mises stresses for outer and inner surfaces of hemisphere is the second characteristic. It describes a general intensity of stress on the surface. In this work Von Mises stresses is calculated for the selected upper finite element located close to the upper point with coordinates  $(0, y, 0)$ . Stress components  $S_{11}$  and  $S_{22}$  are given as a property of deformed material as well. Compressive stress is observed in all the cases.

### 4.1 One-layer structure analysis

The one-layer structure is considered in this section. The magnitude of load is 0.4 MPa. Figure 13 presents the simulated results of case aa. The fixed upper point with the coordinates  $(0, 100, 0)$ (mm) is the point of detecting deformation magnitude. With boundary conditions of case aa the upper point moves down in negative direction along y-axis for

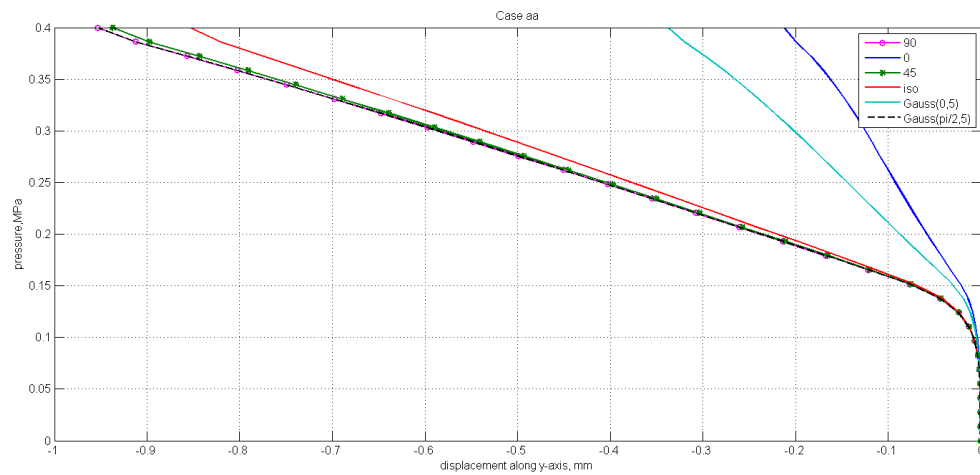


**Figure 13.** Deformation in case aa.

all given orientation angles. As it can be seen, the material with 0 degrees orientation angles is deformed with the smallest absolute value equal to 0.21 (dark blue line). Materials with 90 degrees orientation angle with and without Gaussian distribution have the biggest magnitude of deformation equal to 0.95 mm.

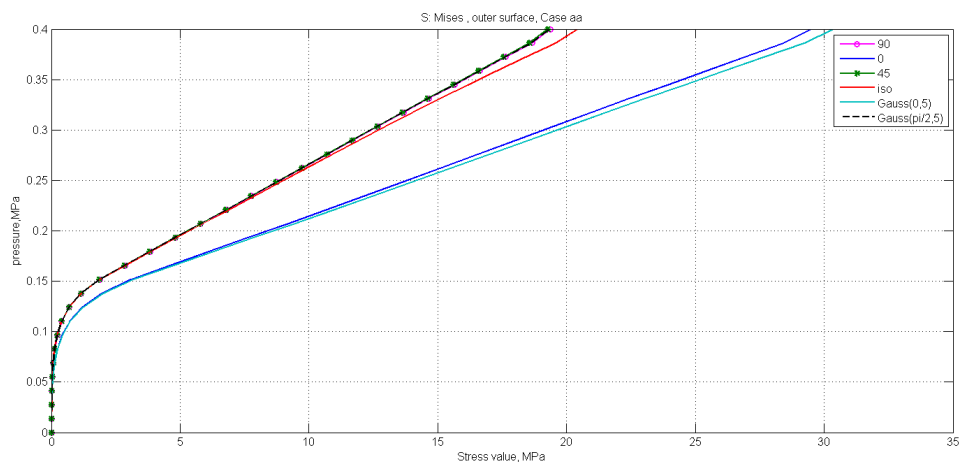
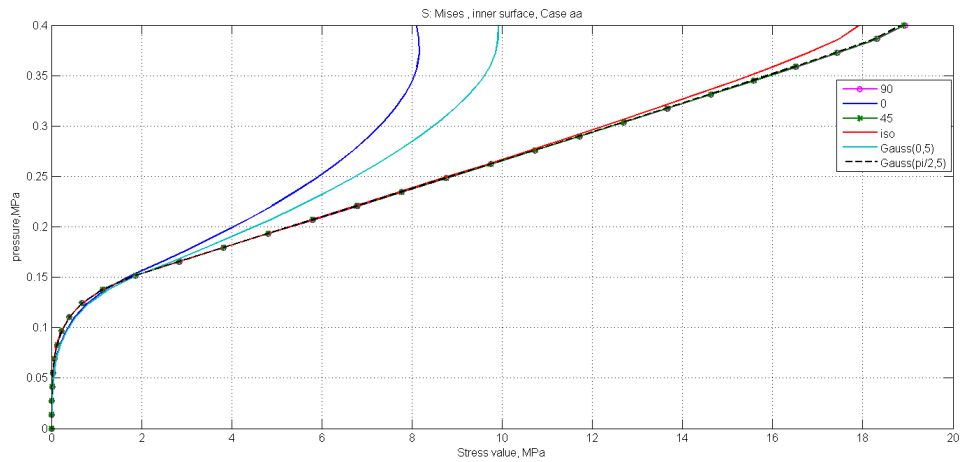


**Figure 14.** Outer surface von Mises stresses in case aa.

Von Mises stresses on outer and inner surfaces of the semisphere are presented in Figures 14 and 15. Stresses are obtained from one specified finite element from the upper part of semisphere. The magnitudes are taken as average for this element ("Centroid" in Abaqus).

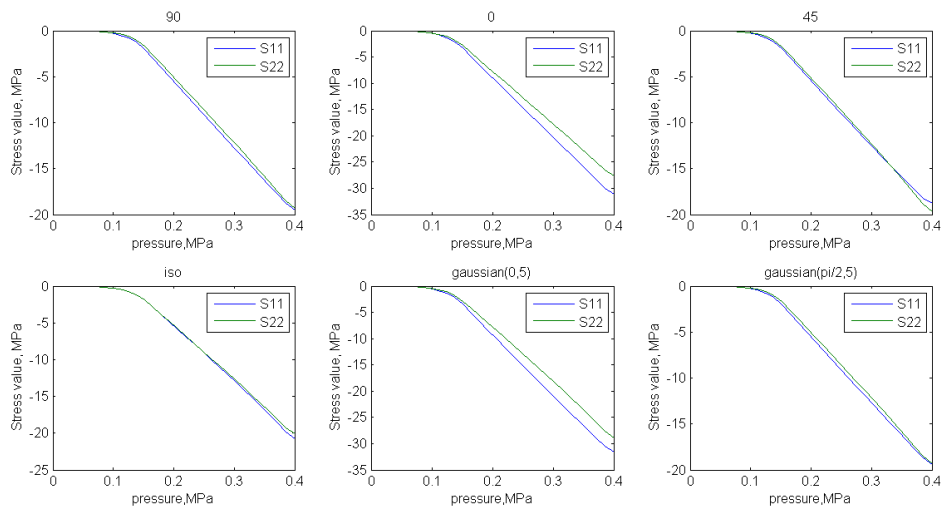
For the outer surfaces the biggest magnitude is obtained for the material with Gaussian distribution with mean 0 degrees orientation angle. It is equal to 29.5 MPa. The material with 0 degrees orientation angle is located close to it. Materials with orientation angle 90 and 45 degrees and Gaussian distribution with mean 90 degrees have the smallest value

of stress together about 19 MPa.



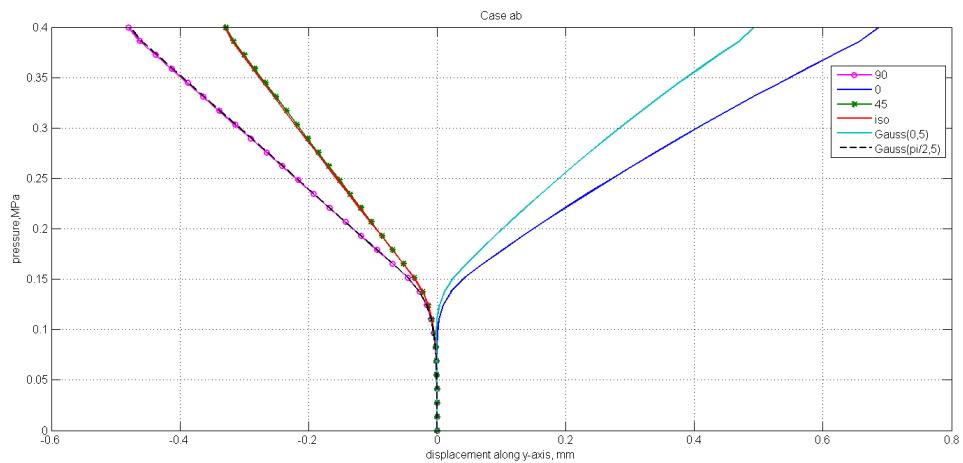
**Figure 15.** Inner surface von Mises stresses in case aa.

For the inner surface (Figure 15) the biggest magnitude of von Mises stresses are obtained with 90 and 45 degree orientation angle and Gaussian distribution with the mean 90 degrees, the values are approximately 19 MPa. Thus, the highest stress on the outer surface corresponds the lowest stress value on the inner surface.



**Figure 16.** Stress components in case aa.

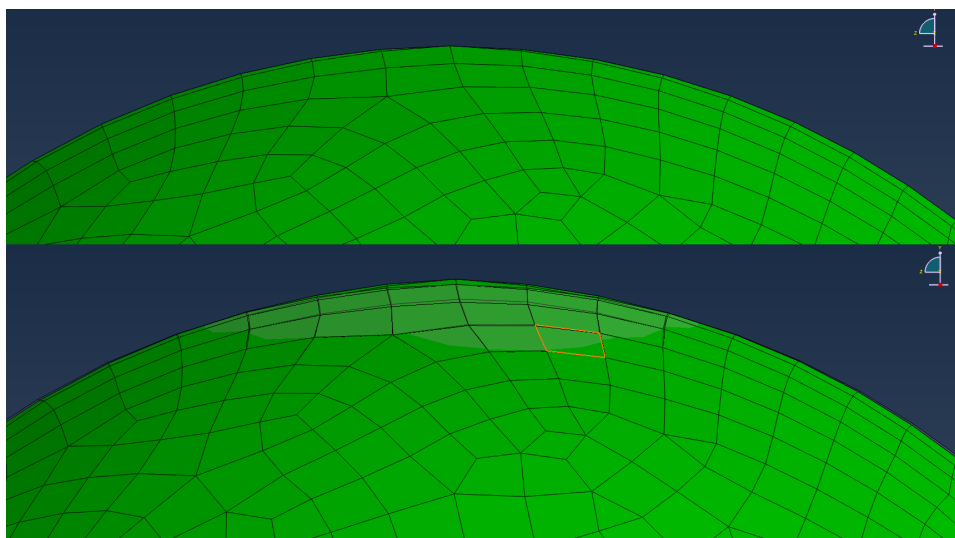
The main components  $S_{11}$  and  $S_{22}$  of stress tensor are considered on the Figure 16. The directions of the  $S_{11}$  and  $S_{22}$  are in the local coordinate system.  $S_{11}$  and  $S_{22}$  can give some characteristic of material behavior. The biggest stress values appear in the body with 0 degree orientation angle and Gaussian distribution with the mean 0 degrees.



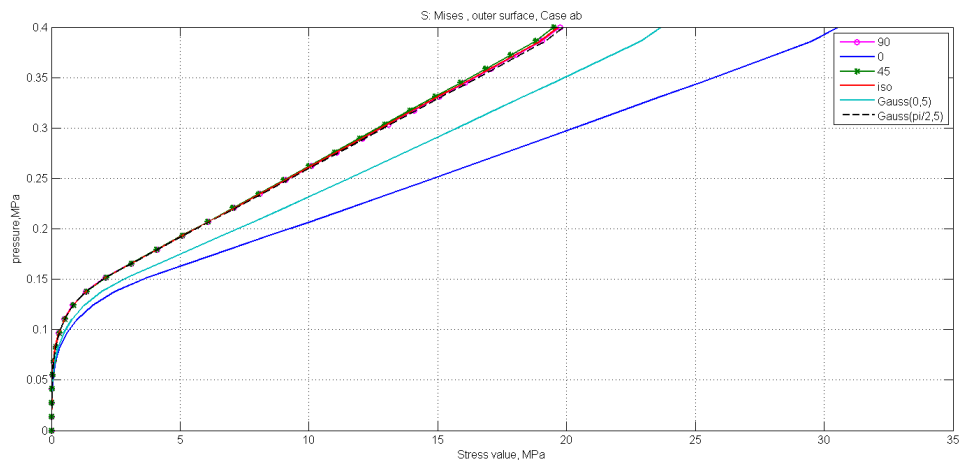
**Figure 17.** Deformation in case ab.

Figure 17 presents the simulated deformations for the case ab. Fixed upper point is the same as in previous case. As load is distributed on the whole surface, deformation can go by different ways. For materials with 0 degree orientation angle and Gaussian distribution with mean 0 degrees the upper point moves in positive direction along the  $y$ -axis with magnitude approximately 0.6 mm. All other materials are deformed in negative direction, the upper point become lower and the magnitude is less. Thus, it can be noticed that material behavior can change significantly because of fiber orientation.

The moving the upper point in positive direction can be illustrated with Figure 18. Light green area comes up after the load, it appears because of distributed load on the whole surface.

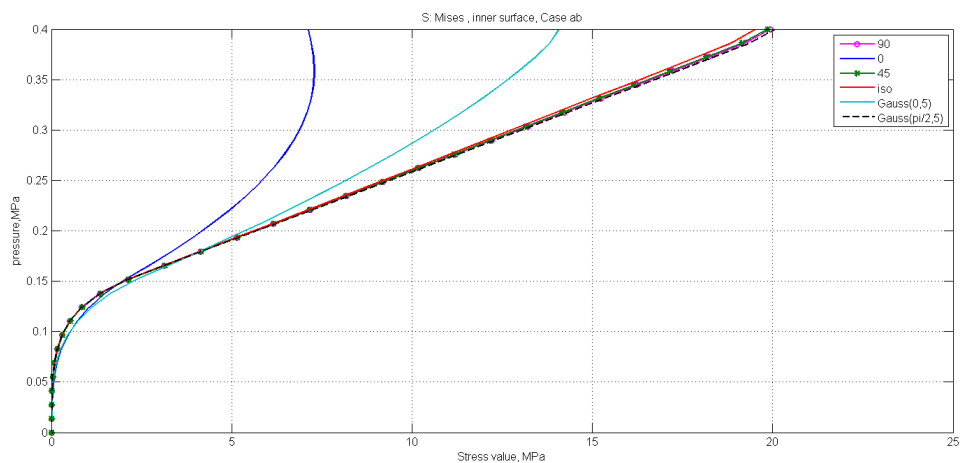


**Figure 18.** Area of deformation in case ab.



**Figure 19.** Outer surface von Mises stresses in case ab.

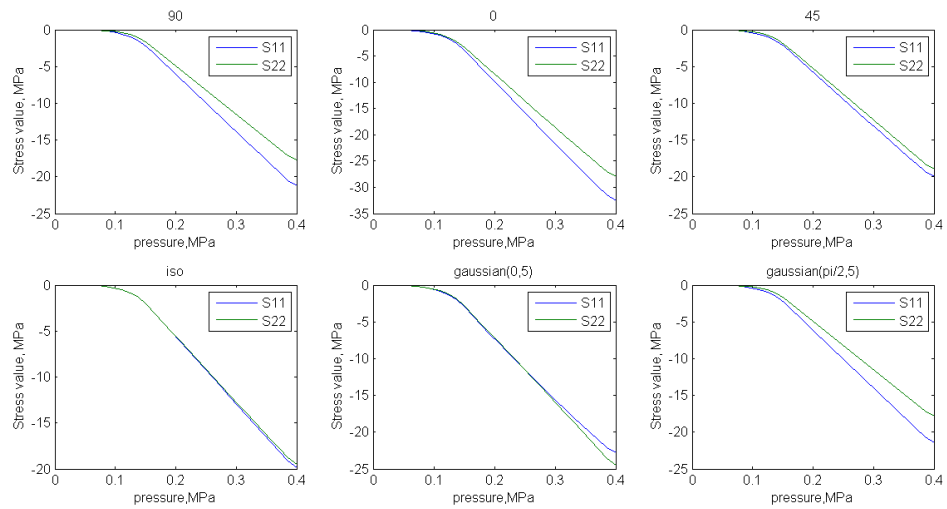
Figure 19 presents the outer surface von Mises stresses in case ab. The biggest stress values are obtained with the material with 0 degree orientation angle and equal to 30.5 MPa, the next value is of material with Gaussian distribution with the mean 0 degree orientation angle. The graphs for all other materials are very close to each other and demonstrate lower values of stress.



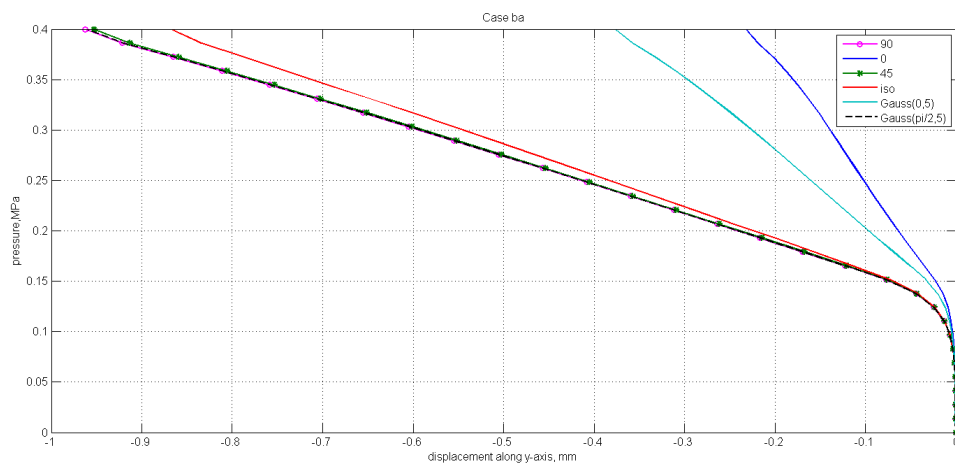
**Figure 20.** Inner surface von Mises stresses in case ab.

Figure 20 presents the inner surface von Mises stresses in case ab. As the stress values for outer surface is bigger then the stress values for inner surface become less.

As can be seen from Figure 21, the biggest main stress components,  $S_{11}$  and  $S_{22}$ , appear in the materials with 0 degree angle orientation and Gaussian distribution with the mean 0 degrees. The lowest stresses are in the materials with 90 and 45 degrees orientation angles.

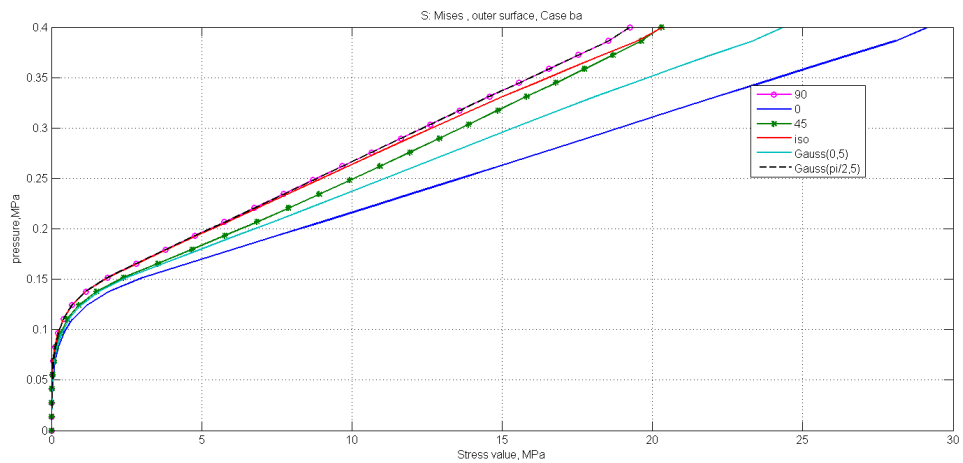


**Figure 21.** Stress components in case ab.



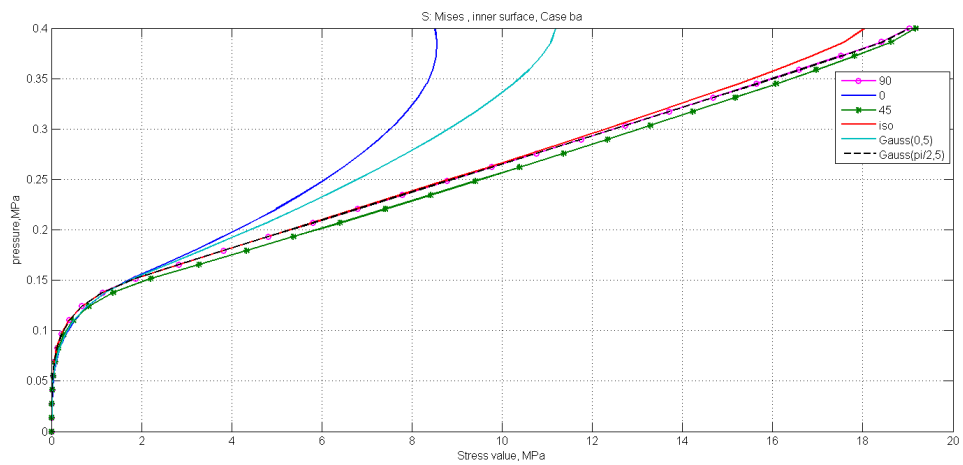
**Figure 22.** Deformation in case ba.

Figure 22 presents the deformation in case ba. In this combination of boundary conditions and load the material with 0 degree orientation angle has the smallest magnitude of strain (0.23 mm). It can be assumed that the fiber orientation angle provides stability in this case.



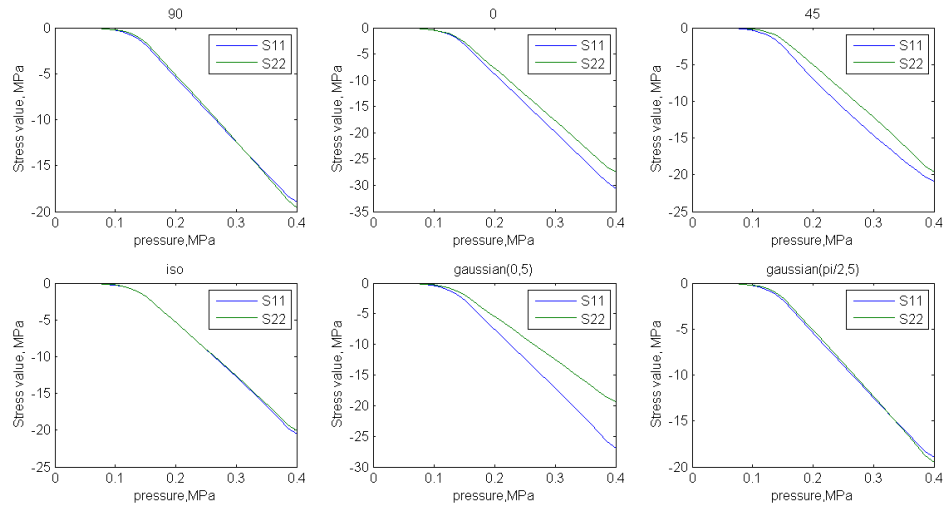
**Figure 23.** Outer surface von Mises stresses in case ba.

Figures 23 and 24 present the outer and inner surface von Mises stresses in case ba. The material with 0 degree orientation shows the biggest stress value on the outer surface (29.2 MPa for an element on the outer surface) and the smallest - on the inner one (8.51 MPa).

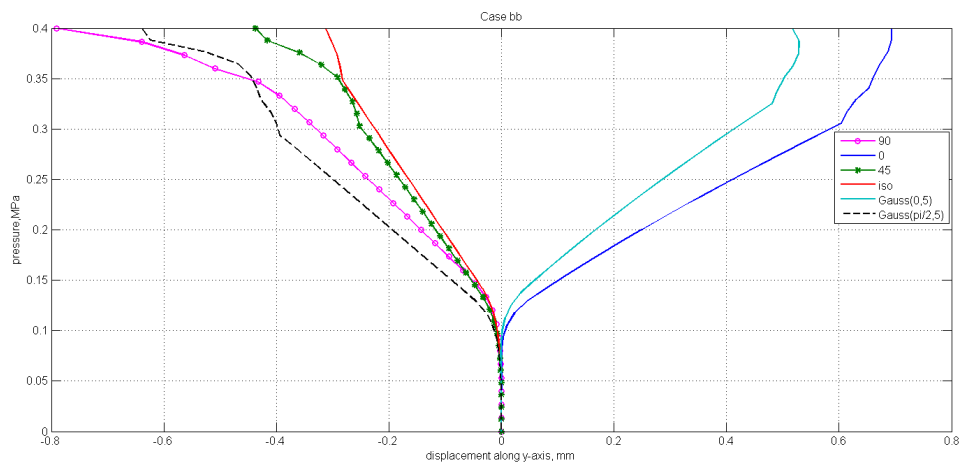


**Figure 24.** Inner surface von Mises stresses in case ba.

The stress components  $S_{11}$  and  $S_{22}$  in the case ba are presented in Figure 25. Materials with orientation angle 0 and Gaussian distribution with mean of 0 degrees have the biggest values of main stress components.

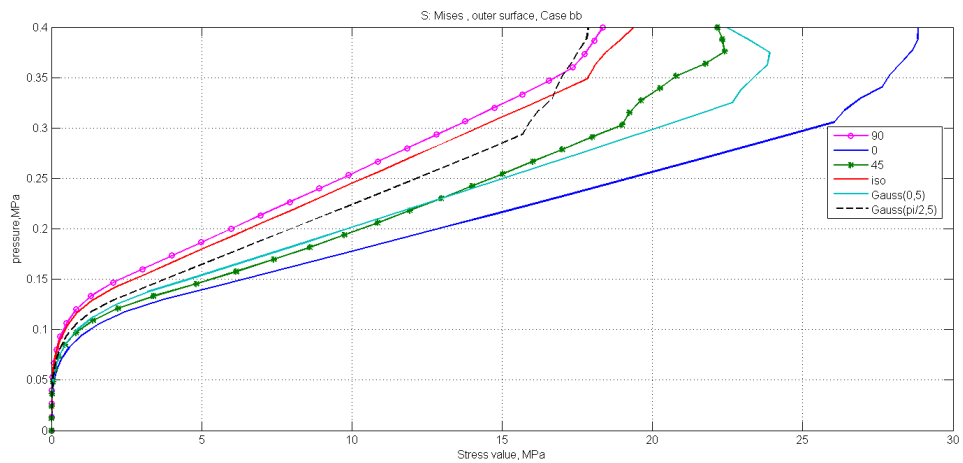


**Figure 25.** Stress components in case ba.



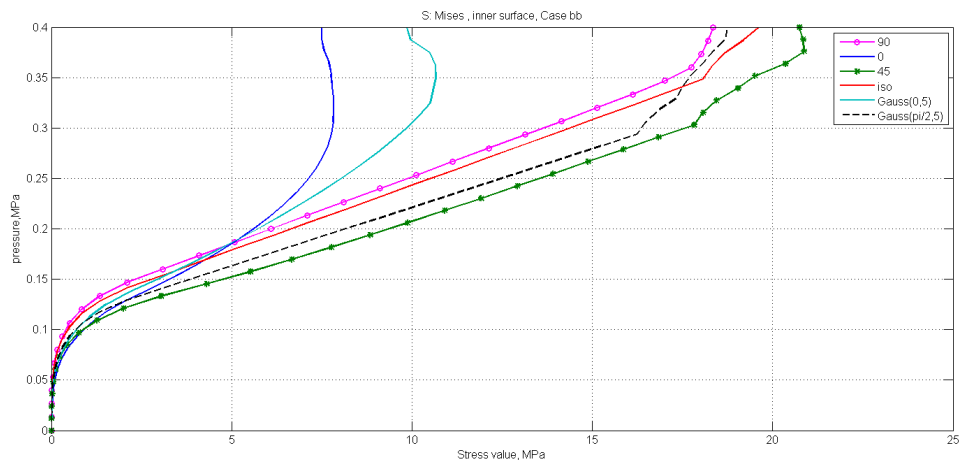
**Figure 26.** Deformation in case bb.

Figure 26 presents the deformation in the case bb. In this case different behavior of materials is observed. Materials with 0 degree orientation angle and Gaussian distribution with the mean 0 degrees demonstrate displacement of upper point in positive direction, in other cases the upper point moves in negative direction along y-axis. The maximal absolute value of strain can be noticed with 0 degree orientation angle (0.6 mm before buckling). As it can be seen, with this combination of boundary conditions and loads buckling process starts when the magnitude of load is bigger than 0.3 MPa.



**Figure 27.** Outer surface von Mises stresses in case bb.

Figure 27 presents the outer surface von Mises stresses in the case bb. The biggest value of stress on outer surface is demonstrated by the 0 orientation angle material (25.6 MPa). On the inner surface of semisphere the biggest magnitude of stress (18 MPa) is obtained with the material with 45 degrees orientation angle (see Figure 28).



**Figure 28.** Inner surface von Mises stresses in case bb.

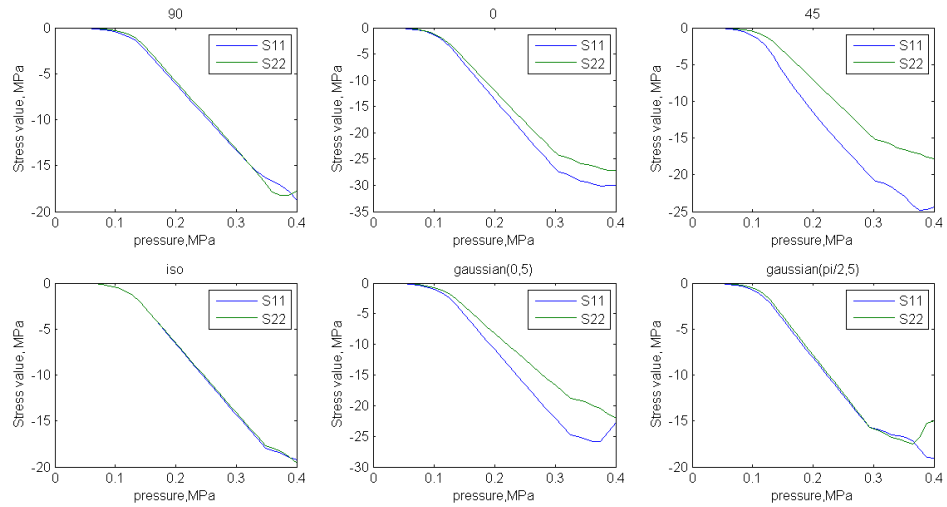


**Figure 29.** Stress distribution components curves in case bb.

As it can be seen on Figure 29, stress components show chaotic behavior for tested materials, it is the start of buckling.

Figure 30 contains scaled contours of displacement along y-axis. The structure shows different behavior with various boundary conditions and loads, it is possible to observe how the structure changes:

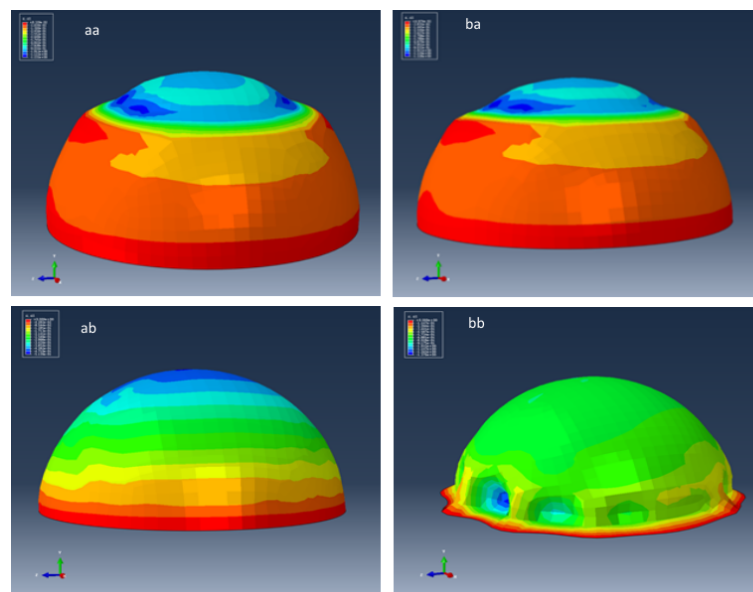


**Figure 30.** Displacement contours for one-layer structure.

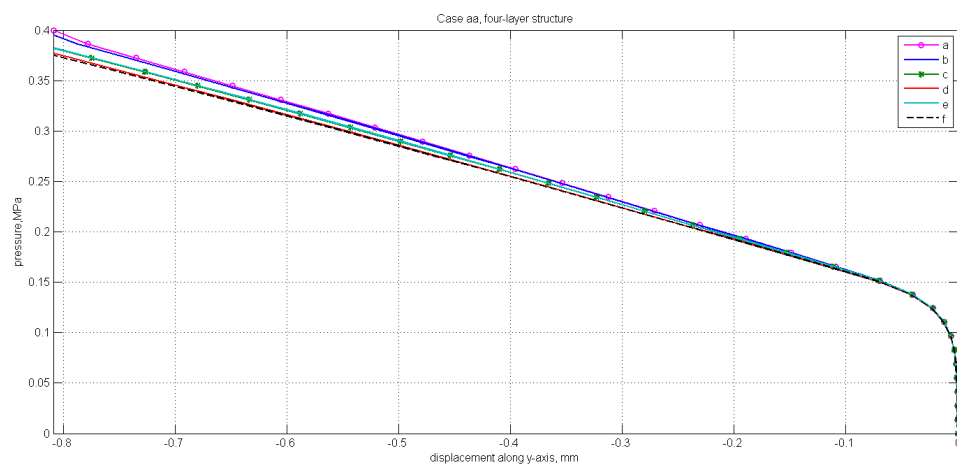
Material with 90 degree orientation angle is considered to compare displacement contours for one-layer structure. Cases aa and ba demonstrate loading the upper area, this area is deformed more than non-loaded surface of semisphere. In case ab all the construction is deformed uniformly. Case bb shows that allowed horizontal displacement on the bottom edge and loading the whole surface leads to buckling early than for other combinations of boundary conditions and loads. Scaled factor in Abaqus is equal to 5.

## 4.2 Four-layer structure analysis

The four-layer structure is considered in this section. The magnitude of load is 0.4 MPa as in the previous analysis. The structure is formed by four layers with orientation angles by Table 1:

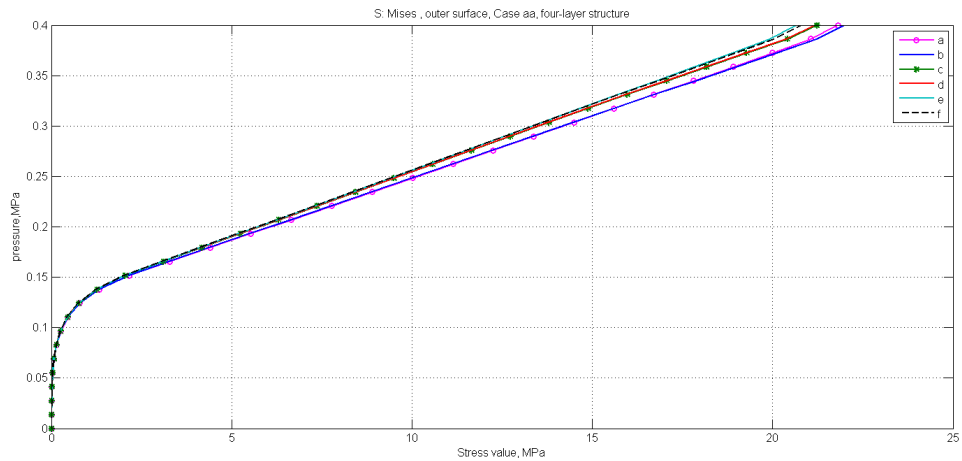
**Table 1.** Four-layer structure organization

| layer number | a  | b  | c  | d  | e  | f  |
|--------------|----|----|----|----|----|----|
| 1            | 90 | 0  | 45 | 45 | 90 | 0  |
| 2            | 0  | 90 | 90 | 0  | 45 | 45 |
| 3            | 0  | 90 | 90 | 0  | 45 | 45 |
| 4            | 90 | 0  | 45 | 45 | 90 | 0  |



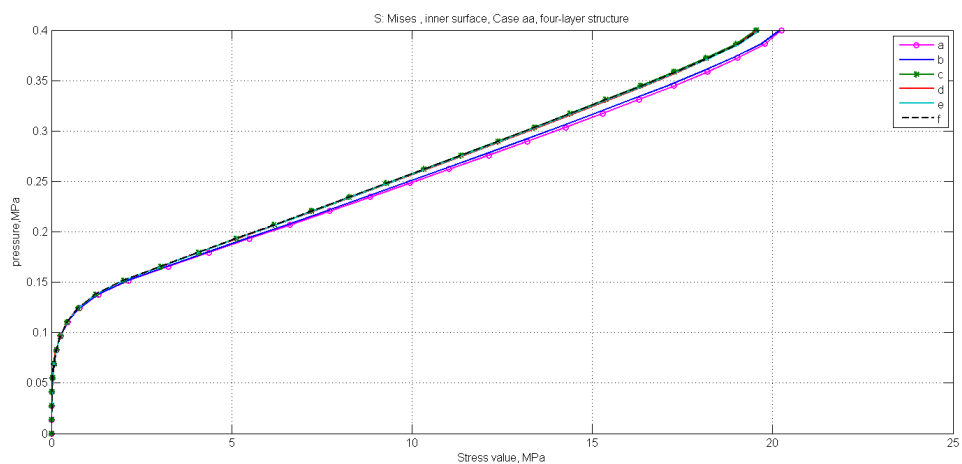
**Figure 31.** Deformation in case aa.

Figure 31 presents the deformations of the different fiber orientation structures. Direction of deformation is the same for all the constructions. The magnitudes are close for all the structures but the biggest value belongs to case f. There are small differences between all cases a-f, material 'a' has the smallest absolute value of the upper point displacement.

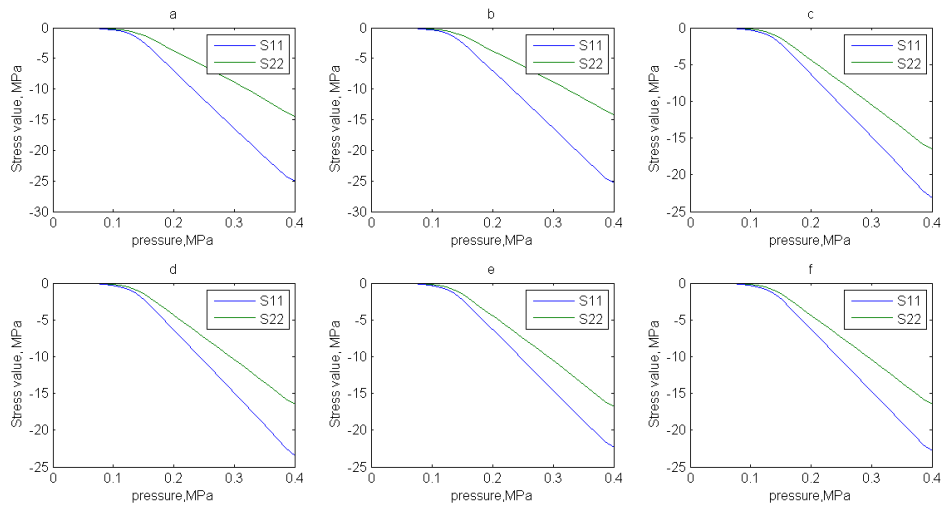


**Figure 32.** Outer surface von Mises stresses in case aa.

Inner and outer surface von Mises stresses are presented in Figures 32 and 33 respectively. The biggest magnitude of von Mises stress appear in the materials a and b for both outer and inner surfaces. Other combinations of orientation angles provide smaller values of stress. In the whole, stress values on the outer surface are around 21-22 MPa while stress values on the inner surface are less and close to 20 MPa.

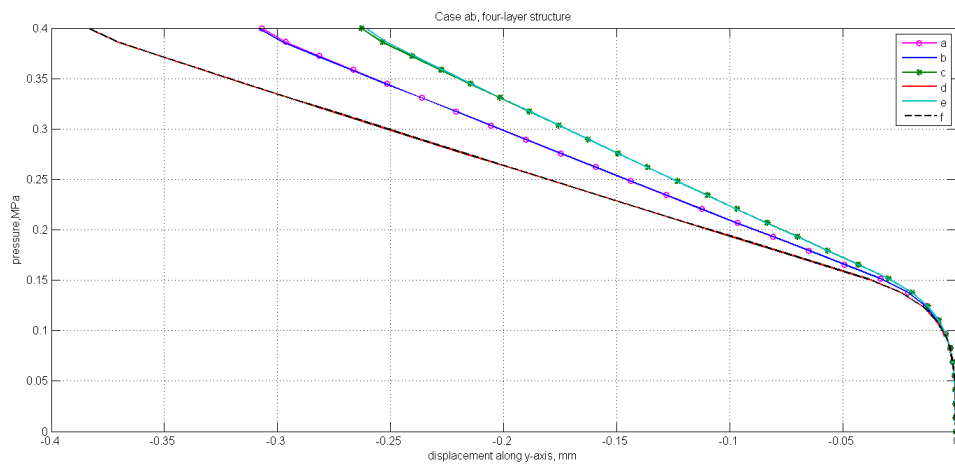


**Figure 33.** Stress distribution curves (Mises) in case aa.



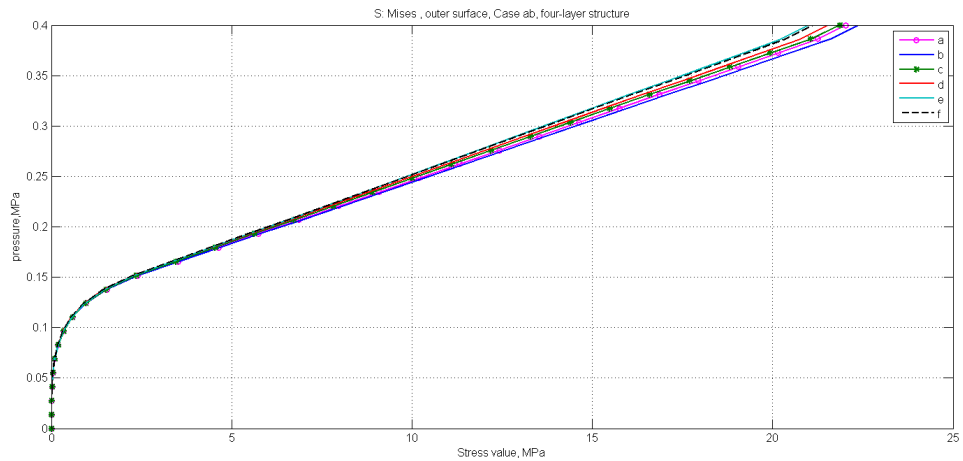
**Figure 34.** Stress components in case aa.

The stress components  $S_{11}$  and  $S_{22}$  are presented in Figure 34. As can be seen, minor differences are obtained with different fiber orientation structures. The biggest absolute values of compressive stress is presented by materials 'a' and 'b'.



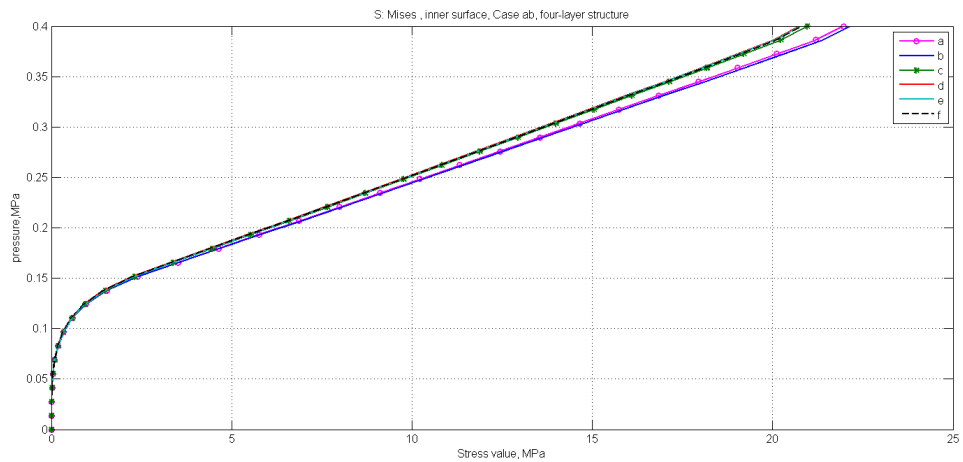
**Figure 35.** Deformation in case ab.

Figure 35 presents the deformations in case ab. As it can be seen, the applied load, distributed on the whole surface of semisphere, gives three pairs of graphs with quite similar behavior and very similar magnitudes of strain for both members of each pair. The fixed upper point changes its location along y-axis in negative direction with absolute values 0.26 mm for materials called c and e, 0.31 mm for a and b, 0.38 mm for d and f.



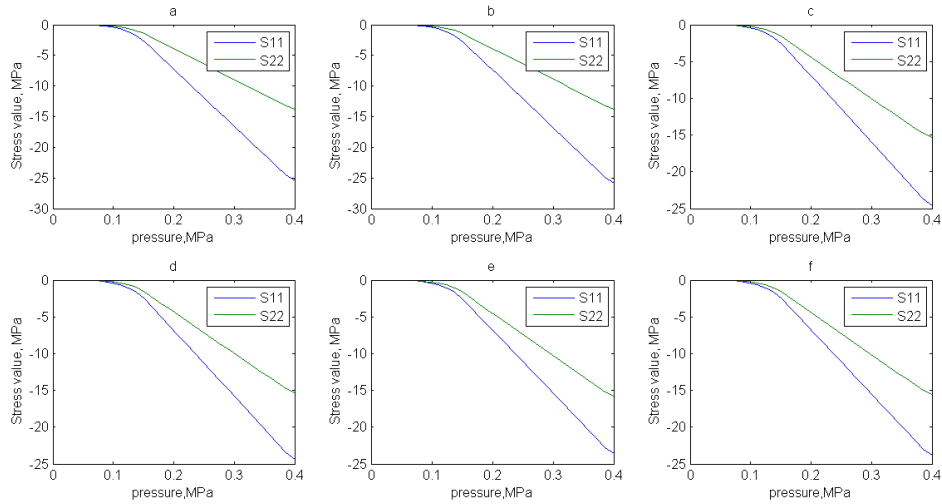
**Figure 36.** Outer surface von Mises stresses in case ab.

Von Mises stresses of the outer surface are different for all materials, as it is shown in Fig.36. They are located between 0.21 and 0.23 MPa, the biggest stress value appears in the material 'b'.



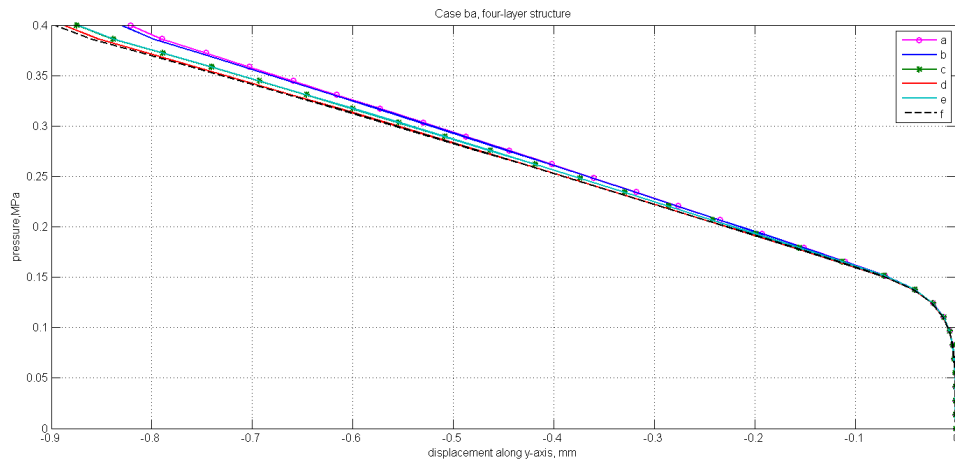
**Figure 37.** Inner surface von Mises stresses in case ab.

For the inner surface (Figure 37) the biggest stress values are observed in materials 'a' and 'b', they are equal to 22 MPa. Other materials provide less intensity of stress and magnitudes are equal approximately to 20-21 MPa.



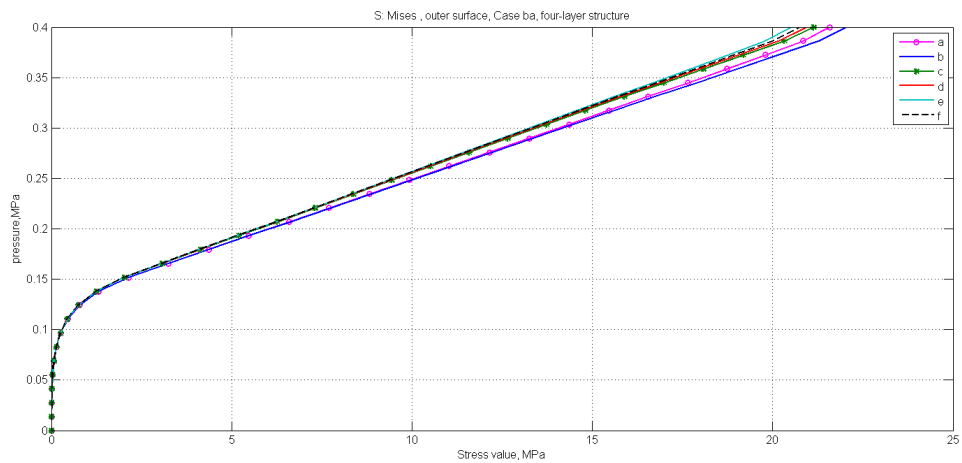
**Figure 38.** Stress components in case ab.

The stress components  $S_{11}$  and  $S_{22}$  are presented in Figure 38. They have some differences obtained with different fiber orientation structures. The biggest absolute values of compressive stress is presented by material 'b'.



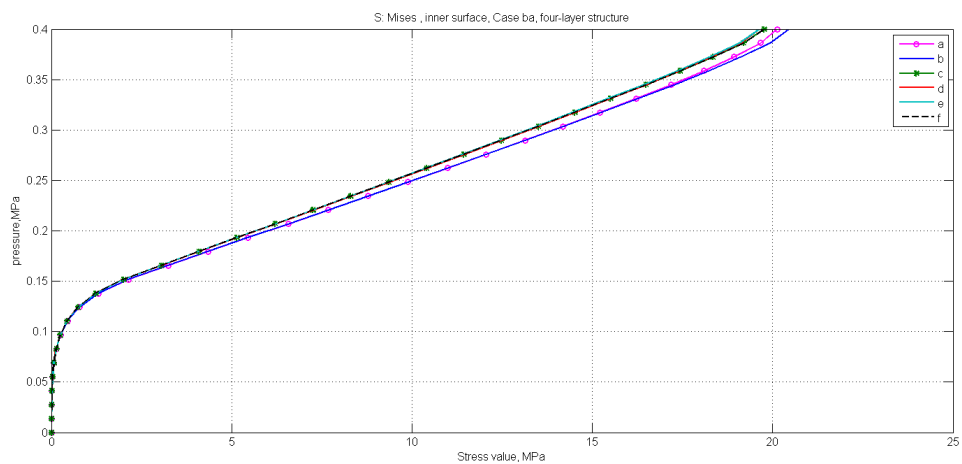
**Figure 39.** Deformation in case ba.

Figure 39 presents the deformations in the case ba. In all cases the fixed upper point moves along y-axis in negative direction. Materials 'a' and 'b' demonstrated the two smallest absolute values (dark blue and pink lines): 0.82 and 0.83 mm respectively. Magnitudes for the other materials are located between 0.85 and 0.90 mm.



**Figure 40.** Outer surface von Mises stresses in case ba.

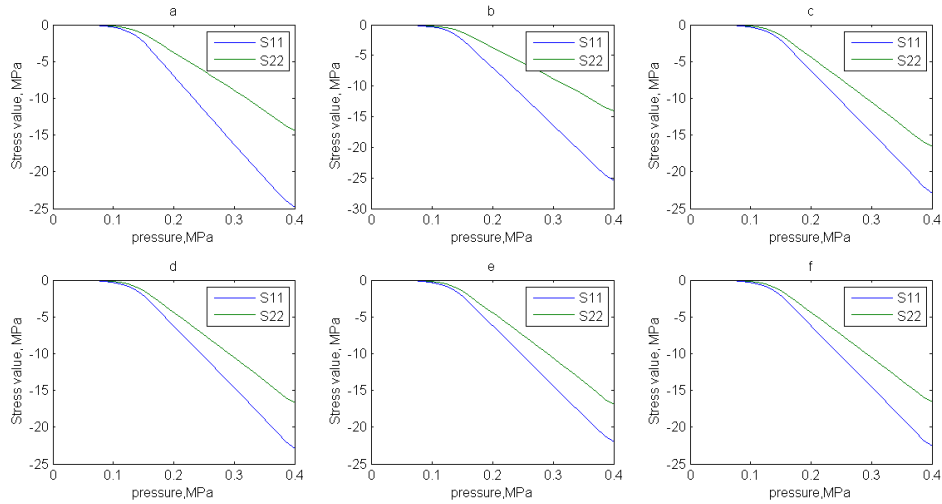
Von Mises stresses for the outer surface in the case ba are presented in Figure 40. The biggest value is observed with material 'b', the next value belongs to material 'a', the smallest - with material 'e'. All the magnitudes for outer surface are located between 20 and 23 MPa.



**Figure 41.** Inner surface von Mises stresses in case ba.

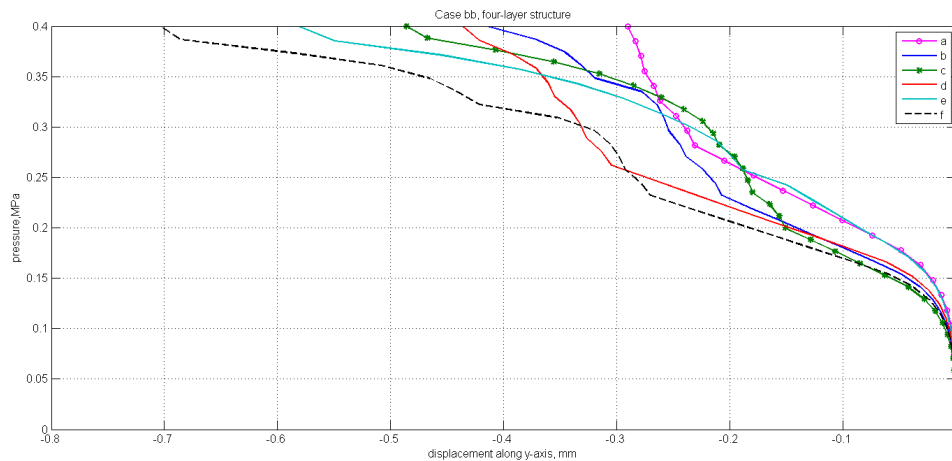
For the inner surface it can be seen on Fig.41 that materials 'b' and 'a' show the two biggest stress value: 20.4 and 20.1 MPa respectively. Other materials have stress values between 19.6 and 19.9 MPa.

The stress components  $S_{11}$  and  $S_{22}$  are presented in Figure 42. The biggest value of  $S_{11}$  component is obtained with material 'b'.



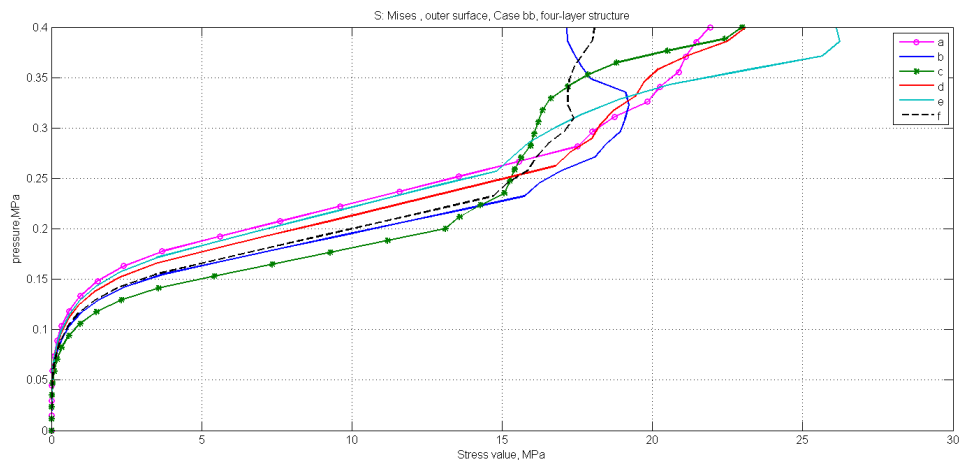
**Figure 42.** Stress components in case ba.

Figure 43 presents the deformations in the case bb. When the pressure is bigger than 0.25 MPa one can see the beginning of buckling process. The graphs show unstable behavior, and the biggest absolute value of strain belongs to material 'f'. The smallest magnitude of displacement is observed with material 'a'.



**Figure 43.** Deformation in case bb.

Analyzing von Mises stress values (Figures 44, 45), it can be said the pressure value 0.25 MPa is 'critical' for this case of boundary conditions and type of load. While pressure magnitude is 0.25 MPa, the biggest stress value belongs to material 'b', but in the final point with pressure 0.4 this material demonstrates the smallest value of stress due to extensive deformation.



**Figure 44.** Outer surface von Mises stresses in case bb.

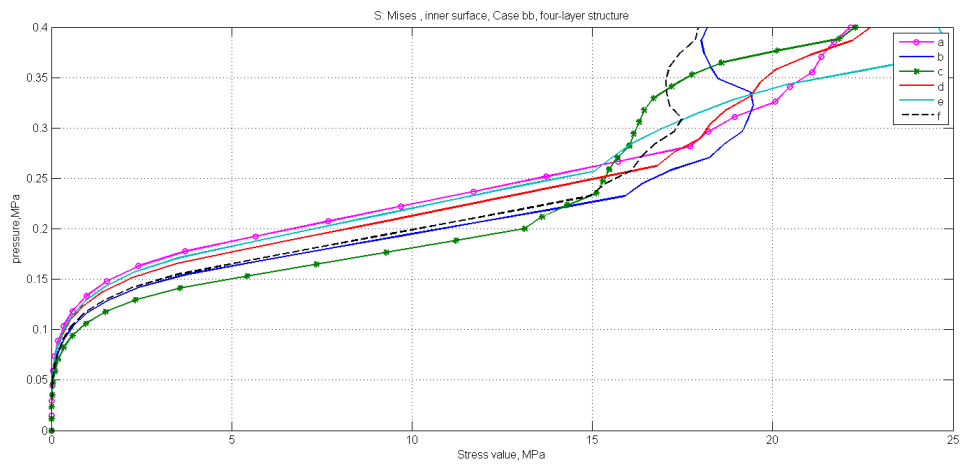


**Figure 45.** Inner surface von Mises stresses in case bb.

Material 'a' has the smallest value of stress when the pressure is 0.25 (Figure 44). Same kind of behavior is obtained for the inner surface (Figure 45).

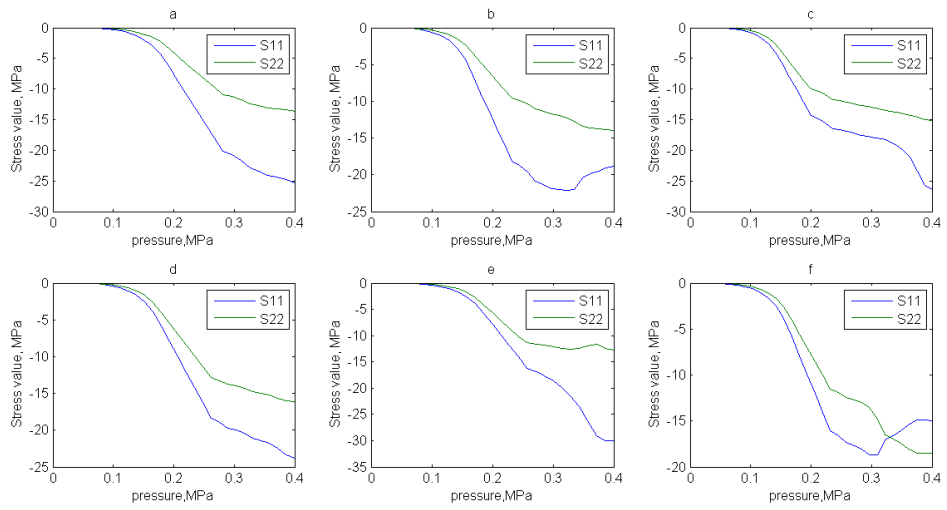


**Figure 46.** Stress components in case bb.

The stress components  $S_{11}$  and  $S_{22}$  are presented in Figure 46. The buckling of the structure can be clearly seen from the results.

The behavior of structures is shown by Figure 47:

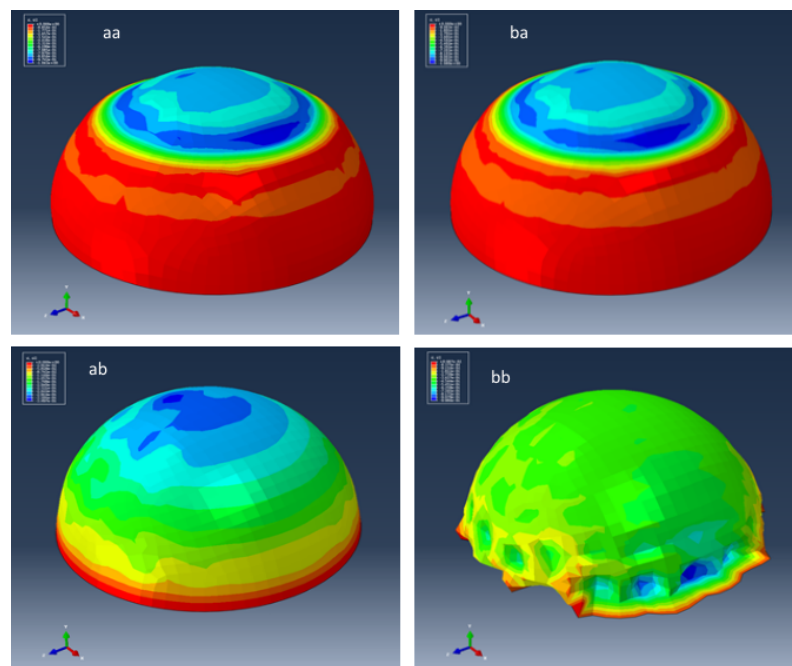


**Figure 47.** Displacement contours for four-layer structure

Material 'a' is considered to compare displacement contours for four-layer structure. Cases aa and ba demonstrate loading the upper area, this area is deformed more than non-loaded surface of semisphere. In case ab all the construction is deformed uniformly. Case bb shows that allowed horizontal displacement on the bottom edge and loading the whole surface leads to buckling early than for other combinations of boundary conditions and loads. Scaled factor in Abaqus is equal to 5.

The numerical results can be combined in the table form as well:

**Table 2.** One-layer structure deformation

| Case | Max value,mm | Orientation angle | Min value, mm | Orientation angle  |
|------|--------------|-------------------|---------------|--------------------|
| aa   | 0.9532       | 90                | 0.2113        | 0                  |
| ab   | 0.6878       | 0                 | 0.3286        | 45                 |
| ba   | 0.9623       | 90                | 0.2317        | 0                  |
| bb   | 0.5832       | 0                 | 0.2321        | isotropic material |

**Table 3.** One-layer structure Von Mises stresses

| Case | Surface | Max value,mm | Orientation angle | Min value, mm | Orientation angle |
|------|---------|--------------|-------------------|---------------|-------------------|
| aa   | outer   | 29.5260      | 0                 | 19.3782       | 90                |
|      | inner   | 18.9315      | 90                | 8.1087        | 0                 |
| ab   | outer   | 30.5511      | 0                 | 19.8543       | 45                |
|      | inner   | 19.7523      | 90                | 7.1309        | 0                 |
| ba   | outer   | 29.1798      | 0                 | 19.0314       | 90                |
|      | inner   | 20.3018      | 45                | 8.5132        | 0                 |
| bb   | outer   | 25.5632      | 0                 | 13.5247       | 90                |
|      | inner   | 18.0231      | 45                | 7.5413        | 0                 |

The follow table contains magnitudes of deformation for four-layer structure, cases are based on Figure 12, orientation of fibers in layers of a construction is based on Table 1:

**Table 4.** Four-layer structure deformation

| Case | Max value,mm | Material orientation | Min value, mm | Material orientation |
|------|--------------|----------------------|---------------|----------------------|
| aa   | 0.8857       | f                    | 0.8094        | a                    |
| ab   | 0.3835       | d                    | 0.2608        | e                    |
| ba   | 0.8966       | f                    | 0.8215        | a                    |
| bb   | 0.1643       | f                    | 0.0844        | e                    |

**Table 5.** Four-layer structure Von Mises stresses

| Case | Surface | Max value,mm | Orientation angle | Min value, mm | Orientation angle |
|------|---------|--------------|-------------------|---------------|-------------------|
| aa   | outer   | 22.0069      | b                 | 20.6626       | e                 |
|      | inner   | 20.2496      | a                 | 19.5413       | c                 |
| ab   | outer   | 22.3947      | b                 | 20.9847       | e                 |
|      | inner   | 22.1677      | b                 | 20.7372       | d                 |
| ba   | outer   | 22.0673      | b                 | 20.5222       | e                 |
|      | inner   | 20.4616      | b                 | 19.6402       | e                 |
| bb   | outer   | 13.1293      | c                 | 5.6053        | a                 |
|      | inner   | 13.1098      | c                 | 5.6594        | a                 |

## 5 CONCLUSIONS

The finite element method was used to analyze six variants of material orientation angles for a single-layer structure and six combinations of orientation angles for a four-layer structure. It can be argued that the orientation angle does affect the amount of deformation during a static analysis of the stress-strain state of the body.

Four selected combinations of boundary conditions and loads affect the construction differently. In cases 'aa' , 'ba' semisphere is deformed mostly in the area of load in the upper part. Case 'ab' provides uniform deformation of a model. Case 'bb' leads to buckling earlier than other combinations of boundary conditions and loads for both one-layer and four-layer structures.

For a single-layer structure in cases 'aa', 'ba' a material with an orientation angle of 90 degrees has shown bigger values of mechanical deformation than other materials. A material with 0 degrees orientation angle has the greatest absolute value of deformation in cases 'ab', 'bb'. For the four-layer structure, the greatest absolute value of deformation was obtained for material f in the cases 'aa', 'ba', 'bb' and material 'd' in the case of 'ab'.

In cases 'aa' and 'ba' a material with an orientation angle of 0 degrees has demonstrated the smallest absolute value of deformation for one-layer structure. In cases 'ab' the smallest absolute value was obtained for a material with an orientation angle of 45 degrees. In case 'bb' an isotropic material without specifying the orientation of paper fibers demonstrates the smallest absolute value of deformation.

The lowest values of deformation for four-layer structure were shown by material 'a' (cases 'aa' and 'ba') and material 'e' (case 'bb').

It can be said that a single-layer material with an orientation angle of 90 degrees and a four-layer material with orientation angles 0 degrees, 45 degrees, 45 degrees, 0 degrees from 1 to 4 layer, respectively, are the least resistant to mechanical deformation.

It can be argued that single-layer materials with an orientation angle of 0 and 45 degrees can be considered as resistant to mechanical deformation but there is strong effect of boundary conditions and loads type. For four layer structure materials with orientation angles 90, 0, 0, 90 degrees and 90, 45, 45, 90 degrees from 1 to 4 layer, respectively, are the most resistant to mechanical deformation.

## 6 REFERENCES

- [1] M. Alava, K. Niskanen, "The physics of paper", Reports on Progress in Physics, vol. 69, pp. 669-723, 2006
- [2] T. Leppänen, J. Sorvari, A.-L. Erkkilä, J. Hämäläinen, "Mathematical modelling of moisture induced out-of-plane deformation of a paper sheet", Modelling and Simulation in Materials Science and Engineering, vol. 13, pp.841-850, 2005.
- [3] Anne Marie Helmenstine. (2017, March 28). What Is the Difference Between Heterogeneous and Homogeneous Mixtures? [Online]. Available: <https://www.thoughtco.com/heterogeneous-and-homogeneous-mixtures-606106>
- [4] J. Sorvari. Modelling Method for Viscoelastic Constitutive Modelling of Paper. PhD thesis, University of Kuopio, 2009.
- [5] M. Karlsson, editor. Papermaking Science and Technology, Part 2: Drying. Fapet Oy, Helsinki, 2000.
- [6] M. Ostoja-Starzewski, D.C. Stahl. "Random Fiber Networks and Special Elastic Orthotropy of Paper", Journal of Elasticity, vol. 60, pp. 131-149, 2000.
- [7] T. Leppänen. Effect of fiber orientation on cockling of paper. PhD thesis, University of Kuopio, Finland, 2007.
- [8] O. C. Zienkiewicz . The Finite Element Method. McGraw-Hill Book Company (UK) Limited, Maidenhead, Berkshire, 1977.
- [9] William N. Findley, James S. Lai, Kasif Onaran, 1989, Creep and relaxation of nonlinear viscoelastic materials : with an introduction to linear viscoelasticity, New York, 402 pp.
- [10] V. I. Feodosiev, 1970, Strength of materials, Moscow, 544 pp.
- [11] J. N. Reddy, 2003, Mechanics of laminated composite plates and shells. Theory and analysis, 2nd edition, CRC Press, 835 pp.
- [12] O. C. Zienkiewicz and R. L. Taylor. The Finite Element Method, Volume 2: Solid Mechanics. Butterworth-Heinemann, Oxford, 2000.

- [13] Available from: [https://en.wikipedia.org/wiki/Finite element method](https://en.wikipedia.org/wiki/Finite_element_method)
- [14] U. Sagdeeva, S. Kopysov, A. Novikov, 2011, Introduction to the finite element method, Izhevsk, 40 pp.
- [15] Available from: <https://habrahabr.ru/post/263597/>
- [16] A. V. Nasedkin, A. A. Nasedkina, 2015, Finite element modeling of coupled problems, Rostov-on-Don, 174 pp.
- [17] Available from: <http://www.me.berkeley.edu/~lwlw/me128/FEMNotes.pdf>
- [18] Available from: <http://illustrations.marin.ntnu.no/structures/analysis/FEM/theory/index.html>
- [19] ABAQUS, 2014. ABAQUS Documentation. Dassault Systemes, Providence, RI, USA.